Titre: Title:	Removal of Contaminant Nanoparticles from Wastewater Produced Via Hydrothermal Carbonization by Spions
Auteur: Author:	Melika Parsapour
Date:	2015
Type:	Mémoire ou thèse / Dissertation or Thesis
Référence: Citation:	Parsapour, M. (2015). Removal of Contaminant Nanoparticles from Wastewater Produced Via Hydrothermal Carbonization by Spions [Master's thesis, École Polytechnique de Montréal]. PolyPublie. https://publications.polymtl.ca/1883/

UNIVERSITÉ DE MONTRÉAL

REMOVAL OF CONTAMINANT NANOPARTICLES FROM WASTEWATER PRODUCED VIA HYDROTHERMAL CARBONIZATION BY SPIONS

MELIKA PARSAPOUR

INSTITUT DE GÉNIE BIOMÉDICAL

ÉCOLE POLYTECHNIQUE DE MONTRÉAL

MÉMOIRE PRÉSENTÉ EN VUE DE L'OBTENTION

DU DIPLÔME DE MAÎTRISE ÈS SCIENCES APPLIQUÉES

(GÉNIE BIOMÉDICAL)

AOÛT 2015

UNIVERSITÉ DE MONTRÉAL

ÉCOLE POLYTECHNIQUE DE MONTRÉAL

Ce mémoire intitulé :

REMOVAL OF CONTAMINANT NANOPARTICLES FROM WASTEWATER PRODUCED VIA HYDROTHERMAL CARBONIZATION BY SPIONS

présenté par : PARSAPOUR Melika

en vue de l'obtention du diplôme de : Maîtrise ès sciences appliquées

a été dûment accepté par le jury d'examen constitué de :

M. COMEAU Yves, Ph. D., président

M. YAHIA L'Hocine, Ph. D., membre et directeur de recherche

Mme BRADL Heike, Ph. D., membre et codirectrice de recherche

M. KHALID Nabil, Ph. D., membre

DEDICATION

To my adored parents whom I owe them all my life,

To my dear husband for all moral support

And my lovely children Saleh and Hosna

ACKNOWLEDGEMENTS

I would like to express my deep appreciate to Professor L'Hocine Yahia for his patience and encouragement during my project and by assisting me in order to fulfill my program.

During the completion of this Thesis, I had an excellent opportunity to work with Dr. Rafaella Oliveira do Nascimento whome I consider a great friend who didn't refuse any favors and helped me through out all stages of these two years.

I sincerely appreciate the help of my co-supervisor, Prof. Heike Bradl for providing the preliminary samples and taking time to read my thesis.

I would like to extend my thanks to all members of our group and others who have encouraged me and provided a friendly environment which was also scientifically stimulating; like Insaf, Karina, Doris, Naziha, Arthur, Aurdia, Juhhan and Noel.

I give my special thanks to Remi, for providing laboratory staff and materials for following up the experimental part of the project, to Patricia the AFM technician of Université de Montréal, to Dr. Murugan for GO preparing and to Amira the general laboratory technician of Université de Montréal.

RÉSUMÉ

La carbonisation hydrothermale (CHT) peut être définie chimiquement comme un processus combiné de déshydratation et de décarboxylation dans un état humide. En bref, ce procédé est réalisé par l'application d'une température élevée (entre 180 à 250°C) et d'une pression (de l'ordre de 2 MPa) pour dégager l'eau de la biomasse et transformer le carbone en biocharbon de haute qualité en l'espace de quelques heures. D'abord la biomasse est chauffée sous forme de solution aqueuse dans un réservoir sous pression jusqu'à ce qu'un procédé exothermique entre en action. Dès ce moment l'exploitation de l'installation ne requiert aucune énergie additionnelle.

En outre, pendant le processus de conversion humide, la forte teneur en résidus est transformée en nanoparticules qui pourraient présenter une nanostructure hétérogène bien définie. Bien que la CHT soit connue depuis des années, on observe un regain d'intérêt envers ce procédé en raison de sa rentabilité et des propriétés intéressantes de ses produits comme le biochar, un produit semblable à l'humus, qui peut être employé pour amender les sols agricoles et stocker le CO_2.

En fait, la CHT a été utilisé pour le traitement des boues et des eaux usées dans certains pays développés tels que l'Allemagne. Aujourd'hui, de nombreux scientifiques continuent à étudier les produits solides de ce procédé tel que le biochar. Ces études concernent la caractérisation physico-chimique et biologique des produits générés par la CHT, ainsi que leur utilisation potentielle. Toutefois, les produits aqueux de la CHT, riches en hydrocarbures dérivés et en nanoparticules (NPs), sont rarement étudiés.

Ainsi, notre objectif est d'étudier les eaux usées générées par la CHT à partir d'une biomasse de glycérine ou de sucre. En outre, nous proposons une nouvelle stratégie de traitement pour éliminer les NPs de ces eaux usées. À cet égard, nous avons utilisés les nanoparticules superparamagnétiques d'oxyde de fer (SPIONs) en raison de leurs propriétés physico-chimiques uniques (propriétés magnétiques, capacité d'absorption, biocompatibilité et éco-compatibilité) pour la décontamination de l'eau et des eaux usées.

Dans ce travail, nous avons synthétisé deux nanocomposites à base de SPIONs pour le retrait magnétique des nanoparticules des eaux usées. Dans le premier cas, nous avons synthétisé des SPIONS recouverts de polyéthylène-glycol (PEG) (SPIONs @ (PEG)). Dans le second cas, nous avons utilisé un procédé de croissance in situ pour produire un nanocomposite de SPIONS et d'oxyde de graphène purifié (OG), (SPIONs / OG), et recouvert par la suite de PEG (20000Da), (SPIONS / OG @ PEG).

Comme les OG contiennent divers groupes fonctionnels comprenant, entre autres, les acides carboxyliques, les hydroxyles et les époxydes, ayant une valence élevée pour l'adsorption de contaminants en raison de leur teneur élevée en oxygène, nous supposons que SPIONS / GO @ PEG améliorent le procédé de décontamination.

Initialement, nous avons caractérisé les SPIONs synthétisés. La spectroscopie infrarouge à transformée de Fourier (FT-IR) a été utilisé pour identifier les groupes fonctionnels présents dans les échantillons de SPIONs. La Microscopie à Force atomique (AFM) et la microscopie électronique à transmission (MET) ont été utilisées pour déterminer la topographie et le diamètre à travers des images de haute résolution des nanocomposites. Enfin la diffusion dynamique de la lumière (DLS) a été utilisée pour évaluer la distribution de la taille des SPIONs dans de l'eau distillée.

En outre, tous les échantillons d'eaux usées ont été caractérisés avant et après le traitement. La FT-IR a été utilisée pour déterminer les groupes fonctionnels dans les échantillons initiaux. La spectroscopie UV-visible (UV-VIS) a été utilisée pour observer l'absorption UV des produits chimiques. La DLS a été utilisée pour mesurer la distribution de la taille et la densité, et finalement la morphologie a été investiguée par une technique d'AFM.

Les SPIONs qui impliquaient du GO en raison de la présence de groupes d'oxyde montrent une structure cristalline mieux ordonnée et une distribution de diamètre plus restreinte. Les échantillons de glycérine traités par SPIONs @ PEG et SPIONs / GO @ PEG ont une réduction de contaminant de 43% et de 38% respectivement. En ce qui concerne les échantillons de sucre, les réductions étaient de 33% et 60% respectivement.

Ainsi, les résultats obtenus confirment la capacité des nanocomposites à éliminer des nano-contaminants à partir d'échantillons d'eaux usées de manière raisonnable. Cependant, la puissance de décontamination des nanocomposites diffère en fonction de la structure chimique de la biomasse initiale.

ABSTRACT

Hydrothermal carbonization (HTC) is a chemical approach that can be defined as a combined dehydration and decarboxylation process in a wet state. Briefly, this process is performed by applying elevated temperature (between 180-250°C) and pressure (arround 2MPa) to convert biomass from aqueous suspension (e.g. sludge, wastewater, natural products, among other) into three different phases and materials products, including biocoal. Further, during the wet conversion process the high residue content is transformed into nanoparticles that could present well-defined or heterogeneous nanostructure. Although HTC was known for years, it has been focused only recently due to exclusive products properties and cost-effective production. In fact, HTC has been used for sludge and wastewater treatment plants in some developed countries such as Germany. Nowadays, many scientific groups still investigate solid products (e.g. biocoal) from HTC. These studies are related to physico-chemical and biological characterization of HTC's generated materials, as well as their potential uses. However, aqueous products from HTC, which are rich in hydrocarbons derivatives and nanoparticles (NPs), are rarely studied. Thereby, our objective is to study the wastewater generated from HTC applied to samples of either glycerin or sugar. Furthermore, we propose a novel treatment strategy to remove the NPs from the wastewater. In this regard, we have used Superparamagnetic Iron Oxide (SPIONs) due to their unique physico-chemical properties (magnetic properties, adsorption capacity, biocompatibility and eco-friendly degradation) for decontamination of water and wastewater. In this regard, we synthesized two different nanocomposites based on SPIONs to carry out the magnetic removal of existent NPs in the wastewater. For the first case, we synthesized polyethylene-glycol (PEG) coated SPIONS (SPIONs@PEG). The second one was a new nanocomposite (SPIONs/GO) obtained from in situ growth of SPIONS over purified graphene oxide (GO), which was afterwards coated with PEG (20000Da), resulting in SPIONs/GO@PEG. As GO has various functional groups that have a high valence for absorption of contaminants due to their oxygen content, we assume that SPIONs/GO@PEG improves the efficiency of the decontamination process compared to SPIONs@PEG alone.

Initially, we have characterized the synthetized SPIONs. Fourier Transform Infrared spectroscopy (FT-IR) was used to identify the present functional groups in the SPIONs samples. Atomic Force Microscopy (AFM) and Transmission Electronic Microscopy (TEM) were used to

determine the topography and diameter size via high resolution images with fine details of the nanocomposites. Finally Dynamic Light Scattering (DLS) was used to evaluate the size distribution of the SPIONs in distilled water.

Also, all wastewater samples were characterized before and after treatment. FT-IR was used to determine the functional groups in initial samples. Ultraviolet-visible spectroscopy (UV-vis) was used to observe the UV absorption of the chemicals. DLS was used for size distribution and density measurement, and morphology investigation was done by AFM technique.

The SPIONs which involved the GO due to the presence of oxidizes groups showed a better ordered crystalline structure and a narrower diameter distribution. The glycerin samples treated by SPIONs@PEG and SPIONs/GO@PEG demonstrated 43% and 38% reduction in contaminant respectively. As for the sugar samples, the reductions were of 33% and 60% respectively.

Thus, the obtained results confirm the capability of the nanocomposites to remove the nano contaminant from wastewater samples reasonably. However, the decontamination power of the nanocomposites differs accordingly to the chemical structure of the initial biomass.

LIST OF SYMBOLS AND ABBREVIATIONS

The list of symbols and abbreviations presents the symbols and abbreviations used in the thesis or dissertation in alphabetical order, along with their meanings. Examples:

AFM	Atomic Force Microscopy
DLS	Dynamic Light Scattering
FT-IR	Fourier Transforms Infrared Spectroscopy
HTC	Hydrothermal carbonization
GO	Graphene oxide
MNPs	Magnetic nanoparticles
NCs	Nanocomposites
NPs	nanoparticles
PEG	polyethylene glycol
SPIONs	Super paramagnetic iron oxide
TEM	Transmission electron microscopy
UV-vis	Ultraviolet-visible spectroscopy
WW	Wastewater

TABLE OF CONTENTS

LIST OF TABLES

LIST OF FIGURES

CHAPTER 1: INTRODUCTION AND OBJECTIVE

1.1 Introduction

These days, water management is one of the dominant controversial issues in its supplying and recycling. The lack of clean water for sanitation and drinking is a common problem in all countries, in particular, the dry ones. Fresh water content is just a small fraction of accessible water, while approximately 70 percent of the earth is covered with water, only 2.5 percent of this water is clean. (Environmental National Geographic 2015). The demand for Water is increasing at a fast rate as a result of the growing population and improved urbanization due to industrial technology. Obviously the resources for potable water in the populated regions is limited and governments attempt to compensate this deficiency for drinking. Distinction between potable water and water for other uses is one of the reputable strategies that is used in many countries such as Germany in many years. For example, managing the wastewater generated by municipal sewage is another source of water supply for cooling systems in industries, agriculture or other consumptions other than drinking. WW (wastewater) with a vast quantity of renewable water for use can have a noticeable amount of beneficial elements such as ions and carbonaceous compounds. It may provide us a new source of energy that can lead to conquering increased problems by WW. As we know the large quantity of WW that has been produced by industrial activities is discharged into affluent water or soil or water systems. Sewage sludge, the residue of WW plants, has been traditionally used for agricultural purposes such as being a source of phosphorous and nitrogen. Besides all valuable agronomic properties, they are often contaminated with a range of hazardous organic and inorganic substances. They may pose a threat to animal, vegetation, ecosystem and humans (Escala, Zumbuhl et al. 2012). This can provide serious problems due to the presence of various kinds of contaminants such as ions, metals, metal oxides, dyes, complex compounds, etc. these produce a poisonious effect on the ecosystem. In order to prevent the problems caused by the entrance of toxic material into the water system, efficiently progressed techniques must be used to control and remove this

contamination from WW and sludge. Unfortunately, there are still more than 90% of sewage easily released into the environment in developing countries, that is causing pollution in causal areas by threatening the animals, plants and human sanitation (Langergraber and Muellegger 2005).

Figure 1-1 Various source of contaminants producing WW collection

There is various biochemical conversion methods to treat the WW that include an aerobic or anaerobic procedure. Among these strategies are to incineration, gasification, and pyrolysis. During these procedures, the feedstock needs to be dried, so the performance of these methods typically takes time and energy. Since most of them are aerobic, they are required to have considerable space to dry feedstock and convert all organic substances into the inorganic part. The conventional treatment for handling the WW problem by the efficient usage of biomass is to produce better combustion for fuel and energy potency (Titirici, Thomas et al. 2007). For instance in Brazil, for several years sugarcane has been converted into ethanol for car fuel or in Sweden since they have focused on the independence of oil import, they used to convert biomass to energy. They found that potential biomass quantities for energy conversion is beneficial due to the production of new alternative potentials for energy (Hagström 2005). Coalification may be one of the natural for biomass but commonly takes place in vast timescales from some hundred to hundred million years for black coal preparation (Titirici, Thomas et al. 2007).

1.2 Objectives

1.2.1 Primary objective

One of the well-known pre-treatment processes for WW and natural biomass is hydrothermal carbonization (HTC). It means wet pyrolysis material in high pressure and moderate temperatures. The wet lingo cellulosic biomass converts efficiently into solid fuel with almost the majority of the initial carbon which includes: approximately 2-11% of gas fraction and 20-37% of carbon in the feedstock which is in liquid form after HTC process (Berge, Ro et al. 2011), and the rest of the parts is in solid form. These are shown in Figure 1-2. The liquid phase of this process involves a considerable section that needs to be investigated more for treatment due to high water content.

The main objective of this work is to reduce nano contaminant of WW samples produced via HTC using the nanomagnetic particles of iron oxides. This approach will be performed by synthesizing nanocomposite of SPIONs, Then treating the WW samples by exposing it with the nanomagnetic particles for a few minutes, which afterwards, by the aid of external lab magnetes will take them out by eliminating the nanocontaminants.

In this research, we focused on the treatment of some WW samples generated by this technique since it may enter into the environment or return into the effluent (?) in safe conditions.

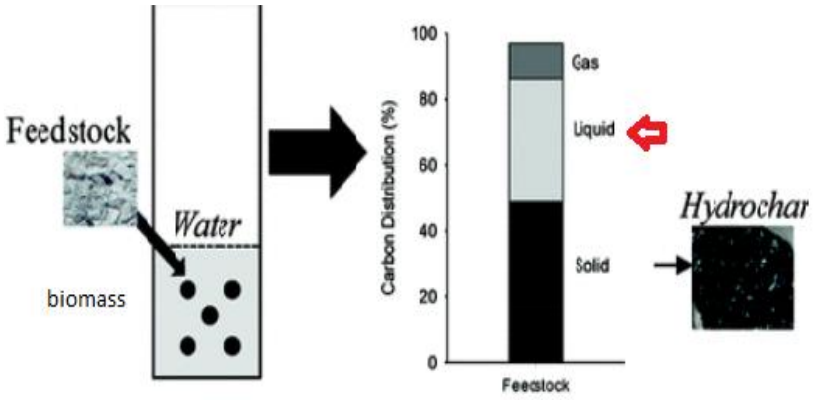

Figure 1-2 Carbon distribution in three phase of HTC product and project objective fraction (Berge, Ro et al. 2011)

1.2.2 Specific objective

According to the literature reviewed in Chapter 2, we defined the feasibility (?) of various contaminants in WW and sludge. Moreover we proposed some nanotechnology approaches for treatment of WW and sludge effluent via HTC by using nanomaterials.

For that purpose, the following specific objectives were considered:

Step 1: Synthesize SPIONs@PEG and SPIONs/GO@PEG by use of hydrochlorate Iron oxide (II) and (III) in presence of nitrogen gas and hydroxide ammonium;

Step 2: Analyze and characterize the fabricated NPs to elucidate the SPIONs structure and morphologies;

Step 3: physico-chemical characterisation of the WW samples (sugar and glycerine) generated by HTC technique;

Step 4: Exposing the synthesized SPIONs@PEG and SPIONs/GO@PEG to the WW samples for treating, then removal of nanosize pollution in presence of magnetic field;

Step 5: Evaluating the NCs functionality by analysing the characteristics of the samples before and after treatment.

In the scope of these specific objectives, different techniques were used to prove the removal competence of fabricated SPIONs for removal nano pollution from WW. The dispersion of SPIONs after exposure with WW was done without employing further technique such as sonication due to possibility for scaling up this method in the industry.

CHAPTER 2: LITERATURE REVIEW

2.1 Hydrothermal carbonization in wastewater and sludge treatment

Among different alternatives for treatment of wastewater and sludge, hydrothermal carbonization (HTC) is one of the favorite procedures that can be done and preserve the intrinsic value of materials which may provide the minimum greenhouse gas production (Berge, Ro et al. 2011). HTC can obtain higher energy efficiency and materials recovery from the used water and sludge, which is why this is the favorite method to generate renewable energy along with fabricating carbonaceous materials with less cyclic unsaturated compounds. In HTC, all procedures are performed at relatively low temperature s(180°- 350° C) and under high pressure (approximately 20 bar). They have reported that in order to prepare char formation via HTC hydrolysis; condensation, decarboxylation, and dehydration reaction occur (Sevilla and Fuertes 2009, Funke and Ziegler 2010).

Heat and pressure are two factors that induce degradation for partial dehydration of organic compounds. Evidently, high pressure accompanies with rising temperature around 200°C during HTC cause conversion of biomass into the carbonaceous materials in aqueous condition. In such wet condition, water also has a significant role for some modifications (Titirici, Thomas et al. 2007, Funke and Ziegler 2010). These changes include physical-chemical variations in materials that happen due to chemical properties of water. Hydrolysis requires lower activation energy than many other thermochemical conversion reactions. In HTC by the aid of water, the reaction can complete with the same degree of conversion efficiency during mild conditions (Funke and Ziegler 2010, Libra, Ro et al. 2011). Obviously the produced composition structure is related to the feedstock thus generating hydrochar composition that is affected by the degradation pathway via HTC. The produced char via HTC may contain attractive surface functionalization patterns, that impact on the potential consequence material for energy-related applications (Sevilla and Fuertes 2009, Titirici and Antonietti 2010). The dehydration occurs through HTC as a chemical reaction in a physical process, the chemical dehydration is eliminating of hydroxyl groups, thus, obtaining the products in lower ratios H/C and O/C. This beneficial dewatering is attributed to HTC. Definitely, lower functional groups such as hydroxyl or carboxyl induce physical

dewatering facilitate (?) (A Funke 2010, M Escala 2012). The drying process by HTC requires less input energy than traditionally reputable methods, for instance, removing one ton of water from sewage sludge needs 800 kWh of thermal energy and 54 kWh of electric energy. Based on these amounts, the calculated total energy for drying sewage sludge is 13 kWh of electrical energy and 164 kWh of thermal energy. This example clearly illustrates that lower required energy input is needed for sewage sludge from HTC in comparison to other established techniques. Sewage sludge has a noticeable quantity of carbonaceous materials and normally has less competence to dewatering due to complicated conditions for easy dewatering. Moisture content in sludge is more than 70% of dry materials so it means most of the released energy from thermal treatment is consumed for dewatering the sludge (Fytili and Zabaniotou 2008). An efficient and economically sound method is to rely on dry matter content (DM) and calorific value of generated product (Escala, Zumbuhl et al. 2012). HTC approach solves this problem by restricting temperature and causing saturated pressure to build up. During HTC process, the biogenetic materials react in an overall exothermic condition, under the net reaction, conclude hydrolysis, dehydration, decarboxylation, polymerization, and aromatization. The described details of reaction are only known for some sample compounds such as cellulose(A Funke 2010). The final productions of HTC are a significant, substantial part of brown coal, high liquid water process and a small portion of gas that is more confined to carbon dioxide. The treatment of HTC condition leads to the formation of the uniform micrometer-sized spheres. Although the diameter of microsphere products regard to the substrate and the reaction modification conditions can modulate, the number of oxygen in a functional groups of the core and the shell are different. This prominate characteristic makes them suitable for the next usage such as enzyme immobilization, and drug delivery, among others (Sevilla and Fuertes 2009).

Since HTC have been using for synthesis the novel carbon – based materials with a wide range of application- probing on all resulted phase of these process is valuable. According to the HTC's outcomes, the produced materials are rich in surface functional groups especially groups content oxygen, with various morphologies. Also, these carbonaceous materials may be mesoporous or microporous so they demonstrate high-interest reactivity. Of course, many parameters are responsible to create final characteristic structures, such as a kind of feedstock, temperature, and pressure. In general, beneficial advantages of HTC is not confined to the

biomass generated, the liquid phase in a high quantity of water with some solved hydrocarbons is another useful approach for HTC plant of WW and sludge.

2.2 What is wastewater

WW is not to confine just to the sewage, all the water that have been used at home, industry, or for agricultural purposes can contain unwilling materials that are potentially capable to change the quality of water. This amount is much more than the water that goes into the drain or sewage water. Approximately 95% of WW content is water and the rest is part made up of solved and dissolved components and compounds. This kind of water can be toxic for ecosystems and human health. Other than the throughout water flow into the sewage system as physical infrastructural plant, there are the other WW sources. Effluent water in the lakes, rivers, landscapes or surface streams are also WW.

Currently, in Canada over 150 billion liters of WW (sewage) is dumped into the water path in untreated or undertreated for each year (Environmental Canada 2015). Evidently, cleaning up of this significant source should be a priority firstly for the environmental safety and human health; secondly for the economic aspects issue seems to be important.

There are some significant questions about the necessary level of testing during treatment of WW for environment safety, in fact this source would reuse for indirect potable purposes. By this approach, the impact of distribution olive mill WW (OMW) on soil properties have been investigated. The obtained results demonstrated that the variations in chemical and mineral properties of the soil can be altered after spreading. These changes are as follows; increasing in phosphorus and potassium concentrations, upraising salinization, changing in the electrical conductivity of soil , and phenol concentration. Therefore, OMW may impact on soil properties by altering the fertility (Zenjari and Nejmeddine 2001). Some professionals believe that, almost other conventional techniques are inadequate for detection of all the microbial and chemical contaminations. They insisted that these compounds can be a significant threat for human health (Crook, MacDonald et al. 1999). Among many concerns regarding health risks, there is information deficiency which associated with the pathogens or unidentified potential of pathogens; moreover the chemical compounds can impact on the qualification of the safety level

of WW before or after the treatment. Thus, identification and detection of the health risks should be proposed before starting elimination and pollution changes.

2.3 Why wastewater requires treatment before returning to the environment?

During urbanization and development with land distribution, elevated new productions and innovated goods, clean water deficiency due to confined sources for supplying is critical problem. Wastewater can be managed to convert re- applicable source of energy and materials for the remedy of the controversial matter. WW may constrain to leftover streaming within the environment for reuse through plants growing or agricultural production. Since, the safe and clean resource of water is restricted, finding some replacement source for the substitution of them seems to be necessary. One of the reputable and accessible stores is used water that possesses a noteworthy amount of water and even may have useful components. Contamination of surface water and groundwater, distributed of WW resources and frequent droughts for extreme global weather patterns induce focusing more on WW treatment Engineering. Obviously, improving WW treatment plan provides treated effluent in acceptable quality, besides other beneficial aspects. For instance, in Atlanta, Ga, this area is the appropriate example of growing population and construction district in the United States (The USGS water science school 2014). The population augmented from 1 million residents in 1950 to 3 million today. Apparently, the accessible source of neat water is not increased but the generated WW, which is contaminated by an enormous mass of new nanostructure substances has altered significantly. In central Mexico, scientists investigated the environmental impact and public health risks associated with irrigation by WW. As they found, metals accumulation in soil may reveal the adverse effect on crops uptake as well as agricultural workers who are exposed to them in the long-term. Also, they showed the elevation of nitrate concentration in groundwater as the potential risk that can be a threat to the humans and the environment (Siebe and Cifuentes 1995).

Municipal WW effluents may have compounds with potential for endocrine disruption. These endocrine-disrupting compound (EDC) can distribute into estrogenic, androgenic and thyroidal

compounds, they could impact on natural function of more than 70000 chemicals (Drewes, Hemming et al. 2005). They have been known for endocrine –disruption potential (Gillesby and Zacharewski 1998). These chemicals may cause a problem by developing their comportment or reproduction of an undesired variety of species. Consequently, the potential for some disease and cancer will increase during imposing with contaminant compounds. On the other hand, the release of volatile organic compound (VOC), toxic air contaminants (TACs), odors, chlorine disinfections and disinfection by-products (DBPs) are some grave concerns among others(Tchobanoglous and Burton 1991).

2.4 Various threat of wastewater and sludge

However, the residue of WW treatment plants have the valuable agronomic properties, such as phosphorus and nitrogen sources. WW and sludge are often contaminated with a broad range of hazardous organic and inorganic substances, which may pose a threat to the environment, animal, and humans (Sterritt and Lester 1980). In most of the countries, WW employing is under the public health supervisor evaluation (Sullivan, Cohn et al. 1973). Sewage WW due to the different usage purposes around the community and urban sources can harm health and the environment (Belgiorno, Rizzo et al. 2007). Also black water (WW from the toilet) and gray water (WW from other sources except the septic toilet) are inevitable constitutions of domestic sewage. Of course, the gray source of WW is less polluted than municipal WW that is also included in black water (Eriksson, Auffarth et al. 2002). There are numerous problems that associate with untreated WW, for instance, chemical and bacteriological quality of septic effluent tanks. The content of gray WW is different from the black one. Also this WW may impact on the contribution of bacteria growth (Brandes 1978). Since the transmission of contaminations is not confined to drinking, inhalation and hand contact, contaminants could be either transferred by the way of distribution of disease factors. Growth within the ecosystem because of micro-organism and different chemicals would be dangerous for all surrounding environment (Dixon, Butler et al. 1999). Domestic WW depends on the source of generation carrier pollutants in different percentage of fertilizers, pathogens, heavy metals, organic compounds, among others. Other useful contaminants from WW are dyes, surfactants, cyclic organic compounds, metals

(particularly heavy metals), pesticides and herbicides, plastic and relative industrial production, and pharmaceutical products. Studying some emerging products such as metabolites, hormones, bacteria and some generated NPs seem important (Jiries, Al Nasir et al. 2002) (Kolpin, Furlong et al. 2002). The presence of some pharmaceutical compounds such as acetaminophen, ibuprofen, and caffeine and furthermore, the existence of hormone in WW are another serious threat for WW and sludge. In these cases, membrane bioreactor(MBR) or some membrane filtration processes by reverse osmosis(RO) and nanofiltration (NF) exhibited active removal (>95%) of the objective analysis(Kim, Cho et al. 2007).

2.4.1 Heavy metal contamination

By improving the novel industrial productions and some non-biodegradable compounds, heavy metals are entering the ecosystem directly or indirectly. Just trace amount of them may cause carcinogenic problems or reveals toxicity conditions for the environment. These metals include zinc, copper, nickel, mercury, cadmium, lead, and chromium. Many of them are capable of combining with other components of sludge to create a new unsafe complex for the ecosystem (Hooda and Alloway 1994). For example, in cement productions industry, or in the main ingredients of cosmetic goods, may find an extensive range of impurity heavy metals such as mercury, lead, arsenic, cadmium or other metals which can induce irritation and penetrate through skin after exposure. Exposure of lead in particular for children and pregnant women could simply influence the central nervous system such as cognitive function and also the regular function of the cardiovascular system (Hu, Shih et al. 2007). Definitely, the toxic level of heavy metals not only showed the adverse effect on human healthy and animals but also demonstrate variation in plants (Prasad 2004). Furthermore, heavy metals contrary of organic waste may be accumulated and deposited in living tissues. This case may present abnormal functions or disease due to the over limited amounts of heavy metals in biological organs (Wan Ngah and Hanafiah 2008). The concentration of heavy metals are non-variable by ordinary technique, WW treatment plant are almost performed in high temperature or firing. So the remaining metals in sludge can reveal desparate side effects by spreading through the environment.

These days, numerous methods have been proposed for removing heavy metals from WW and sludge. Although membrane filtration, electrochemical technologies, chemical precipitation and ion exchange are some proposed technique for heavy metals removal, adsorption due to high efficiency, low cost, and easy operation is preferred (Mishra, Singh et al. 1996). Weng et al. determined influence of temperature and sludge sources on changing the evolution of As, Cd, Cr, Ni, Rb and Zn because of their abundant presence in the sludge (Weng, Ma et al. 2014). Salehi et al. have evaluated the concentration of heavy metals in the sludge of the industrial area and compared with standard conditions the heavy metals levels in ordinary residential sludge produced from WW. They demonstrated presence of high level of lead in industrial city sludge that lead to restricted use of them for agricultural fertilizer (Salehi, Mirghaffari et al. 2013).

2.4.2 Drugs

The comprehensive productions of medication goods are the reason for emerging new demands for curing, causing the presence of these substances in a vast range. They can enter into the effluent system by sewage distribution systems. When people take the medication, just some part of the defined dose is absorbed by the human body, and the rest of the fraction is excreted into the sewage system. These complicated compounds are almost case non-degraded and flow through the municipal sewage system. The pharmaceutical materials can leak into the groundwater or find a path toward surface effluent. Therefore they may cause various contamination degree depending on the kind of substances. The disposal of unwanted or expired drugs is another source of contaminants which enter the waste stream by throwing them into trash or pouring them down the sink or flushing them down the toilet. In all cases they eventually end up returning to landfills and the environment (Kotchen, Kallaos et al. 2009). This great concern is referred to the emission of these pharmaceuticals including antibiotics via soil, air, and water. They may induce the emergence of new bacteria which is empowered by increasing their persistence. Figure 2-1 shows the partial chemical structure of antibiotics. The bacteria can almost survive themselves and withstand antibiotics via mutation to convert persistent bacteria.

Afterwards, they will not answer ordinary antibacterial treatment. For this reason, the control of the bacterial mutation acceleration can impact the effectiveness of antibiotics (Andersson 2003)

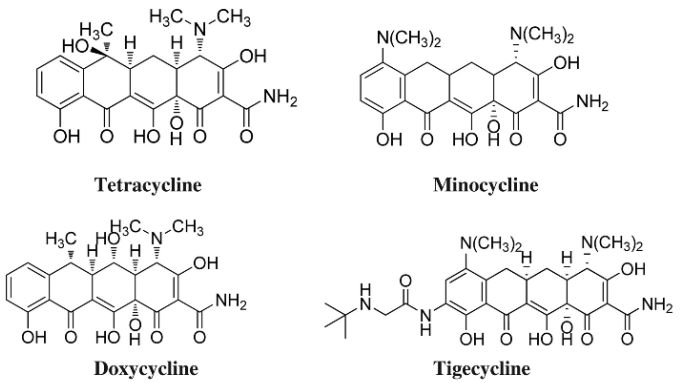

Figure 2-1 Some chemical structural of antibiotics

Some researchers evaluated the amount of illicit drugs concentration in WW including amphetamine-type stimulants, cocaine, MDMA (ecstasy), nicotine and cocaine metabolites. The occurrence of these were particularly observed after Christmas and New Year holidays (Huerta-Fontela, Galceran et al. 2008). By this approach, WW and sludge have a high potential for circulating antibiotics and chemical compounds to alter the microbial ecosystem. For instance, while the resistance of bacteria is increasing during genetic variation events, a biological residue with originated organisms can remain and react with other agents in WW and produced sludge (Baquero, Martínez et al. 2008). Thus addressing whole pharmaceutical chemical composition in WW before interacting with the human body seems to be essential.

2.4.3 Pesticides and herbicide

Herbicides are the principal organic chemicals that are widely used in agricultural applications. During various anthropogenic activities in agricultural actions. Pesticides and phenolic compounds are the known materials, showing environmental hazards associated with WW. In spring unusually high concentration of these chemicals are found in German rivers by passing through various pathways (Nitschke∗ and Schüssler 1998). So they threaten public health due to

their bio-recalcitrant nature and high poisonousness (Eriksson, Baun et al. 2007) (Ahmed, Rasul et al. 2011). Some of the pesticides are introduced in Figure 2-2.

Exposure of pesticides such as DDT derivatives can associate with pancreatic cancer (Garabrant, Held et al. 1992). Another side effect of pesticide is to be at risk of chronic exposure for advanced disease. Some of the reputable diseases which have been observed are leukemia, lymphomas, brain tumors, or testicular cancers (Zahm, and Mary 1998).

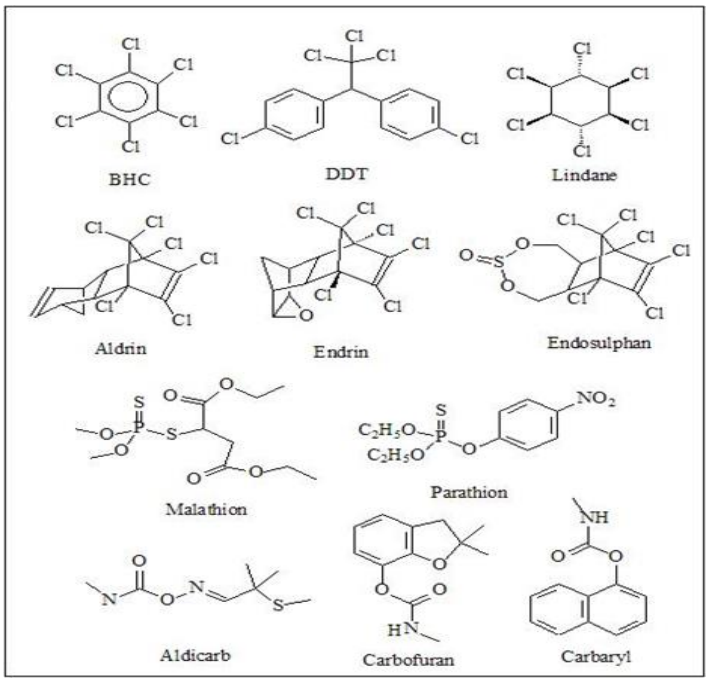

Figure 2-2 Chemical structures of some pesticide

Furthermore, persistence of these organic compounds can effectively impact the ecosystem through contaminating water supplies such as the surface and the ground water (Eriksson, Baun et al. 2007). Although the conventional WW treatment plants are capable of removing most of the pollutants, these systems require an additional step to release or destroy these bio-recalcitrant contaminants from WW effluent in low concentration (Arques, Amat et al. 2007). The presence of excess nitrogenated and phosphorus compounds in the effluent water help to feed more algal bloom, which starves fishes by consuming oxygen content. It would create an environmental

crisis. Moreover potentially, algal blooms can change the coastal ecosystems that consequently are a threat to human health (Vaccari 2009).

Wittmer et al. evaluated the significant presence of pesticides and biocides in surface water by considering all these substances. As they stated, they may mobilize and transport from a local point to other sites, thus emerging aquatic environmental threat. They comprehensively investigated the contribution of biocide inputs from urban drainage systems and agricultural lands into surface waters (Wittmer, Bader et al. 2010). The chemical families of pesticide almost include chlorine and phosphor accompanied with a complicated organic group that may involve aromatic hydrocarbons. Prominent families of herbicides include benzoic acid, and some phenoxy derivatives. The central high load of herbicides that contributes to the effluent system in Germany during spring and early fall which is related to atrazine and desethylatrazine. More than 80% of all herbicides load in urban WW treatment plant constitutes diuron that is used for weed control (Nitschke and Schüssler 1998).

2.4.4 Dyes

The widespread disposal of industrial WW includes complex organic dyes with unsaturated aromatic ring. The dyestuff poses a serious problem to WW for instance textile industry products with a considerable level of dye and toxic floating solid materials (Pandey, Singh et al. 2007). It is evaluated that 5000 tons of dying materials are discharged into the ecosystem each year. These toxic materials may demonstrate hazardous effects such as oxygen deficiency in water (Pirkarami, Olya et al. 2013). This issue should be mentioned that around 15% of the textile dyes which are released during the use of production lines flow toward effluents (Lazar 2005). Biodegradation of this kind of compounds owing to their stability and aromatic molecular structures are difficult, Figure 2-3 shows the chemical structure of some of them. These poisonous chemical reagents can show toxic effect on the health of humans by inducing tumors, cancers, or a number of allergies and on the growth of bacteria, protozoans, plant and animals (Bakshi and Sharma 2003) (Sponza 2002, Moawad, El–Rahim et al. 2003).

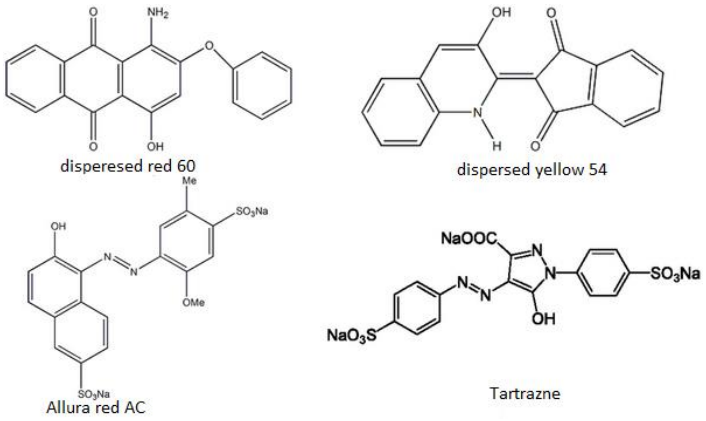

Figure 2-3 Some typically dispersed dyes

A Common Strategy for WW treatment including sedimentation, chemical analysis, biological method, and chemo-coagulation takes much time and are not capable of degrading them completely. Also, the adsorbents are not reusable. The other approaches such as photo catalyst, ozonation, and photo Fenton are expensive and uneconomical (Can, Kobya et al. 2006). Therefore, finding the practical and economical way for the treatment of these contaminations from WW by respect for the energy and the materials is needed. Activated carbon is known for one of the best dye adsorbents for effluent treatment (Mittal, Kaur et al. 2009).

2.4.5 Complex compound

Moreover the hazardous contaminants that are categorized to focus on awareness as priority contaminant compounds, there still are emerging comprise products exist for investigating, they have high probability for adverse effect on the environment. These products involve human and veterinary pharmaceuticals, surfactant and residue of them, plasticizer and relative industrial additives, pesticides and phenolic compounds, metabolites, hormones and bacteria (Petrović, Gonzalez et al. 2003). The environmental risks which associate with the manufacture, employing and disposal of these chemicals. They are used in polymers, textiles, pharmaceuticals, and cosmetic productions. For instance, detergent effluent can induce significant environmental pollutions due to soaps and all their toxic ingredients. Influencing the permeate quality of

flowing and even high rejection of detergents have probably occurred by agglomeration of surfactant particles and the components of pre-micelles and micelles. It seems, these huge molecular structures not only impact on the toxicity of WW but also may cause various problems for WW treatment (Kowalska, Kabsch-Korbutowicz et al. 2005).

In some reports the effluent concentration of pharmaceutical substances in WW treatment plants are measured. According to surveys done by Ternes (Ternes 1998) in Germany, WW treatment plant removal of clofibric acid (CA), a lipid regulator metabolites, and carbamazepine (CBZ), and antiepileptic agents, are done poorly. They demonstrated that just 51% CA and 7% CBZ were eliminated after treatment. So it would be a concern to fade away these pharmaceutical chemicals into the water after passing the WW treatment plant. There are some other contaminant compounds in WW such as estrone (E1), benzophenone (BZP), ibuprofen (IBP), diclofenac (DCP), carbamazepine (CBZ).The chemical structure of some of them is shown in Figure 2-4.

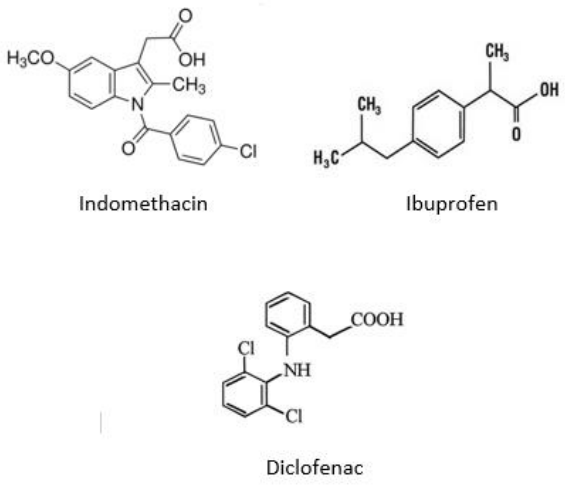

Figure 2-4 Some pharmaceutical chemical structure

Urase and Kikuta studied the activated sludge for removal of three estrogens, two endocrine disrupters, and pharmaceuticals. They traced them in the WW treatment plant by determining the pH and concentration. They found that acidic pharmaceuticals such as clofibric acid, ibuprofen, diclofenac remained in the water as ions, thus sludge adsorption can not remove them (Urase and Kikuta 2005). There are some other hypothesis to degrade these elements from WW during

treatment plants like UV irritation or Fenton reaction, which requires more various complexes with unaddressed questions through WW treatment plans. Still there should be relevant essays done to evaluate their impacts in the sewage.

2.5 WHO and regulatory monitoring

World health report (WHO) is a constitution with direct authority for health within the United Nation system. It provides leadership on global health issues for all technical support and setting up standards and norms. As WHO/UNICEF reports from 54 low and middle-income countries, 38% of people were lacking access rudimentary level of water, whereas 19% suffering from sanitation deficiency and 35% were deprived of appropriate conditions for hand washing (World health Organization 2015). They have some regulatory aspect for using WW, excreta and the gray water in a safe condition to reduce freshwater consumption, and reduce health risks for downstream communities. WHO's program for water and WW is to monitor water and WW for sanitation and hygiene and assess the related risks associated with health – based targets. In 2006 WHO published a guideline to provide standard regulations for WWs and excreta safety in agricultural and aquacultural field.

2.6 Resource recovery from wastewater and sludge

There is a consensus among researchers that the WW and sludge are not waste and have the potential to convert the valuable resources and alternative energy. Due to the economic and environmental constraints, finding an efficient alternative to efficiently use the immense mass of sludge seems necessary. Producing solid fuel from sludge by HTC process is a favorable approach that may reduce the dependency to fossil fuels. As mentioned before, HTC may resolve the problems associated with sludge disposal by conversion to the new energetic resources. In this sight, resource recovery of WW and sludge may change the valuable new sources of energy.

These resources include solid materials (metal, nutrients, phosphate, and hydrocarbons), water, biogas, and energy.

The potential for energy recovery from sludge depends on the composition that may content a mixture of organic compounds (somehow volatile matter), inorganic materials (metals and inert materials) and a noticeable amount of water. However volatile solids are subdivided into components that are correlated to readily degradability, these involve energy of the waste (Tyagi and Lo 2013).

2.7 Contaminants in wastewater

There are various compounds, and element pollutants that are the primary focus of interest and awareness. Some of these compounds are less and more relevant for the industrial waste that can be emitted by the surface WW and sludge. Since, all contaminants have the potential to become environmental problems or widespread emerging unregulated consensus pollution requires appropriate measurements. Following them detection and elimination of the dominant source of contamination are expected. The WW generated from sugar industries bear a high degree of pollution load. WW from sugar industry, if discharged without treatment, poses pollution problems in both aquatic and terrestrial ecosystems. Also, sugar industry WW when not treated completely produces unpleasant smells after being released into the environment. All vegetable oils can be processed into biodiesel (Pousa et al., 2007). Glycerin is considered the main byproduct generated in the production of biodiesel, which represent approximately 10% of the total volume of produced biodiesel (Dasari, Kiatsimkul et al., 2005).

The glycerin obtained by the trans esterification of vegetable oils (biodiesel production) has impurities such as water, alkali catalyst, unreacted alcohol, fatty acids, and other compounds.

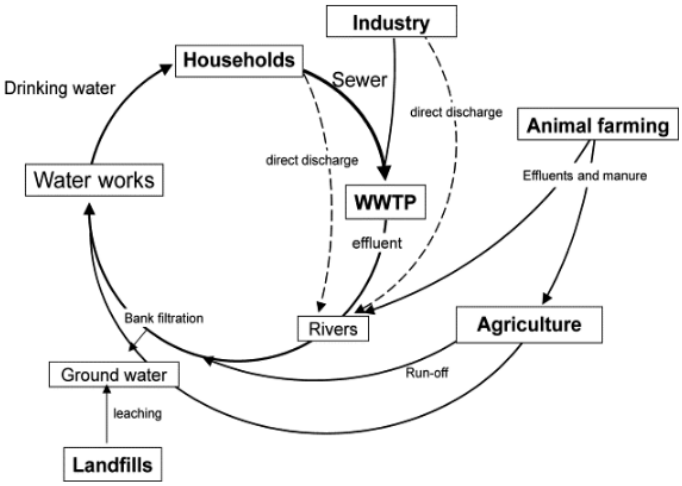

Figure 2-5 Partially component of the closed water cycle to show re-use potable indirectly (Petrović, Gonzalez et al. 2003)

Typically WW is generated by comprehensive sources such as domestic, municipal, agricultural and industrial. These vast contaminations may enter the WW effluent. Figure 2-5 shows typical WW cycle that may come to water potable distribution net indirectly. In fact, certain synthetic and natural compounds may reveal and perform like natural hormones through endocrine systems. These substances are now known as endocrine disrupting compounds (EDCs). They can cause various adverse effects on the human body system and the wildlife, as well as many pharmaceuticals and personal care products (PPCPs) that have been observed on different surfaces and ground water. Considering this issue seems significant that the amount of them are traced (Snyder, Westerhoff et al. 2003). Discharging them into the environment may cause detrimental effects after being conveyed into the human body.

2.8 Application of Nanostructure for wastewater treatment plant

Nanotechnology opens up the tremendous field of useful, beneficial application to human and environment by manufacturing nanoscale materials. Their concrete structure causes disparate chemical and physical properties. In the WW and sludge treatment issue, nanomaterials (NMs) have appeared so more efficient, fast and economic performance for clean-up sludge and WW in comparison with traditional materials (Chen, Crittenden et al. 2005). NMs due to having high

proportional of surface area to volume of particle and sequestration characteristics of specific contamination abstract attention of the researchers. Also, having a particular surface area in NP leads unique adsorption properties pertain to different distribution of reactive surface sites and the abnormal surface region. For instance, iron oxide and titanium oxide in nano-scale are suitable for metal removal from contaminated water. In water purification purpose four classes of NPs are being evaluated (1) dendrimers (2) metal-containing NPs (3) zeolite (4) carbonaceous NMs. Their exclusive physicochemical properties make them different from other materials (Tiwari, Behari et al. 2008).They may deploy quickly to the sludge or slurry reactors for treatment by different layers of waste including solid wastes, contaminated sludge or sediments part of the WW. Definitely, NPs can be anchored to another matrix such as zeolite or activated coal to improve efficiency for WW treatment (Zhang 2003). Zero- valence iron as a reactive agent for WW treatment have been used for easy accessibility, low-cost and reasonable effectiveness for degradation contaminants. Nanoscale of iron particles reveals operative functions in transformation and detoxification of various environmental contaminations as shown in Table 1, they could be pesticides with chlorine group content, or some chlorinated organics. North America utilized metallic iron for remediation of groundwater over a decade, through on reducing or degradation chlorinated organic compounds to low toxic one. Since, zero valence iron exhibits high tendency to donate electron in water to convert iron (II). Many significant contaminants such as chlorinated hydrocarbon, azo dyes or nitroaromatic compounds intend to take the released electron, ultimately these products degrade to the corresponding hydrocarbon. (Ma and Zhang 2008).

$$Fe^{\circ} \rightarrow Fe^{+2} + 2e^{-}$$

$$R\,Cl + H^{+} + Fe^{\circ} \rightarrow R\,H + Fe^{+2} + Cl^{-}$$

Metallic iron can be used to remove pollution from WW by reduction or sorption process; these waste compounds can halogenate hydrocarbon, heavy metals, dyes, pesticides, and herbicides. Although ionic iron produces as a by-product during reaction remains in the environment without any changes, it would generate some intermediate compounds. In this regard, it may convert some toxic chemical materials into less or non-toxic compounds (Junyapoon 2005).

Table 1 Common contaminants that can be removed via nanoscale iron particles (Li et al. 2006)

Chlorinated methanes	Trihalomethanes
Carbon tetrachloride (CCl_4)	Bromoform ($CHBr_3$)
Chloroform ($CHCl_3$)	Dibromochloromethane ($CHBr_2Cl$)
Dichloromethane (CH_2Cl_2)	Dichlorobromomethane ($CHBrCl_2$)
Chloromethane (CH_3Cl)	Chlorinated ethenes
Chlorinated benzenes	Tetrachloroethene (C_2Cl_4)
Hexachlorobenzene (C_6Cl_6)	Trichloroethene (C_2HCl_3)
Pentachlorobenzene (C_6HCl_5)	*cis*-Dichloroethene ($C_2H_2Cl_2$)
Tetrachlorobenzenes ($C_6H_2Cl_4$)	*trans*-Dichloroethene ($C2H_2Cl_2$)
Trichlorobenzenes ($C_6H_3Cl_3$)	1,1-Dichloroethene ($C_2H_2Cl_2$)
Dichlorobenzenes ($C_6H_4Cl_2$)	Vinyl chloride (C_2H_3Cl)
Chlorobenzene (C_6H_5Cl)	Other polychlorinated hydrocarbons
Pesticides	PCBs
DDT ($C1_4H_9Cl_5$)	Dioxins
Lindane ($C_6H_6Cl_6$)	Pentachlorophenol (C_6HCl_5O)
Organic dyes	other organic contaminants
Orange II ($C_{16}H_{11}N_2NaO_4S$)	N-nitrosodimethylamine (NDMA)
Chrysoidine ($C1_2H_{13}ClN_4$)	TNT ($C_7H_5N_3O_6$)
Tropaeolin O ($C_{12}H_9N_2NaO_5S$)	Inorganic anions acid
OrangeDichromate	(Cr_2O^{2-})
Acid Red Arsenic	(AsO_3^{-4})
Heavy metal ions	Perchlorate (ClO_4^-)
Mercury (Hg^2+)	Nitrate (NO^-)
Nickel	(Ni^{2+})
Silver	(Ag^+)

2.8.1 Iron oxide NMs

The application of iron oxide nanoparticle for in vitro diagnostics returns to more than 40 years ago (Gilchrist, Medal et al. 1957). In last near decade, many scientists investigated on several type of iron oxides and their potential for performance and properties. Among them may refer to magnetic particles (maghemite, γ-Fe_2O_3, magnetite, Fe_3O_4, especially with 5-20 nm diameter). Fe_3O_4 is one of the best candidate in biocompatibility (Paterson 1992).The magnetic nanoparticle shows an extensive removal capacity, fast kinetic and high reactivity for eliminating contaminant. Most of their properties associated with the small size particle and high surface area. Magnetite iron oxide has cubic inverse spinal structure, oxygen's place in fcc closed packing while Fe cations are occupying tetrahedral and octahedral sites (Dwight, Klein et al. 1985). The magnetite with the proper surface coating can be dispersed in a homogeneous form suspension (Wang, Hussain et al. 2001). In the absence of any surface coating, magnetite particles because of high hydrophobic surface intend to agglomeration form and to make large cluster. In this case, the size of nanoparticle mass increase and it may impact on the active surface sites. Since the NPs have large surface area, the surrounded high free energy shows the main role for its configuration thus may conduct some changes for the stability state. Subsequently, the clusters, show strong magnetic dipole-dipole attraction similar to ferromagnetic behavior (Hamley 2003). Van der Waals force causes the particles magnetically attaching each other by usual flocculation thus surface modification is often requisite. Aggregated particles demonstrate less activity for removal as well as magnetic properties on the basis of reduction their surface area. For prevention this occurrence, proper coating is required to have the adequately stabilized iron oxide. Surface coating not only can enhance the stability of NPs but also reduce their willing to make clusters in agglomerated shape. Some stabilizer such as a surfactant or a polymer is desired during synthesis magnetite to prevent aggregation of the nanosize particulate (Gupta and Gupta 2005).

2.8.1.1 Iron oxide for wastewater treatment

Nowadays, application of iron oxide NMs has much abstract attention due to the exclusive magnetic properties and the possibility of modification of surface beside the great biocompatibility. During the effort on combat remediating of WW and sludge, iron oxide NMs with low toxicity and neutral chemical effect demonstrate a remarkable potential in combination with biotechnology (Gupta and Gupta 2005). Magnetism is a unique physical property that can impact on water purification for removal existed contaminations in water; Hence it may enhance environmental cleanup by adsorption procedure (Ambashta and Sillanpää 2010). Adsorption process with the magnetic separation can exhibit unique performance for water treatment or environmental cleanup (Mahdavian and Mirrahimi 2010). Current, iron oxide NMs application can be divided into two groups: (a) employing iron oxide NMs for removal efficiency enhancement as a nano sorbent material. (b) iron oxide NMs which are utilized as a photocatalyst convertor or a starter of the reaction. Based on this information, many technologies use both of these characterizes (Xu, Zeng et al. 2012). In this study, the nano sorbent properties are the intention.

One of the main WW pollutions that leads to great concern for environment, plants, animals, and human being are heavy metals. Iron oxides magnetic NMs have convenient tendency for magnetic separation of heavy metals from WW (Hu, Wang et al. 2010). The iron oxide illustrates excellent superiority for rapid, economical and efficient removal of metal ions from WW effluents (Xu, Zeng et al. 2012).

Here, it should be mentioned that surface modification of the NPs causes to enhance the active adsorption on their surface. Moreover surface coating by NMs not only helps the stabilization and less aggregation of NPs but also may induce the selective attachment of materials for uptake from WW. Various types of functionalized materials have been used on the surface of NMs for heavy metals removal, for example, the carbon- encapsulated magnetic NPs Cu^{+2} and Cd^{+2} adsorption (Bystrzejewski, Pyrzyńska et al. 2009).

Super paramagnetic Fe_3O_4 NPs are used to eliminate phenolic and aniline compounds from acidic or neutral condition solution by catalysis properties (Pan, Pan et al. 2009).

2.8.1.1.1 The relation between contaminants removal and magnetite nanoparticle size

The large contaminants removal capacity, fast chemical reaction and physical interaction of the magnetic NPs are principal advantages of these NPs for treatment. When the size of particles decreases, the active sites for interaction with other particle improve. In this case, total required mass for treatment automatically drops along with the significant effectiveness active sites increase. That means, it would be cost effective for application even for industries. However, there are some presented reports that have demonstrated the average removal capacity doesn't change with decreasing the particle size (tratnyek, p. g. nanotechnology for environmental cleanup 2006),(Yean et al. 2005). This point should be mentioned, all physical and chemical interfaces usually occur in solid –liquid phase. By this approach, the probability of interaction may reduce by decreasing the size of the particle. In interaction deficiency for particles, obtaining not significant removal activity is normal anticipation for results. Therefore, the removal performance is closely related to the size and surface area of the magnetite NPs.

2.8.1.1.2 Magnetic nanoparticle recovery

Particle size is the variable factor that may impact on efficiency and qualification of the particles manipulation by a magnetic field. Increasing the size of magnetite iron oxide can direct influence by reduction in reactivity and in NPs active sites that leads to changes in removal capacity in consequence (Papaefthymiou, G.C., 2009). The method of synthesized NPs may define the magnetic NPs properties. To obtain the balance between the conditions for NPs properties, considering the state of existing NPs properties in a fluid seems important.

To the economical application of iron oxide NPs for water and WW, the power of external magnet for providing magnetic field should be noticed. In some case, the magnetic field produced by a hand-held magnet would be strong enough to manipulate and take out the MNPs covered by NPs. On the other hand, smaller size of NPs, more strength magnet is need to provide adequate attraction for conquering other forces such as drag and Brownian motion (Tratnyek

and Johnson,2006). A stronger magnetic field like coil conductor or superconducting magnet is required for providing sufficient strength in desired temperature for removing and recovery the MNPs after treatment in the industry. With the conception possibility of magnetic recovery, the particles under magnetic field intend to the aggregation. By some technique such as sonication may separate the particles. Moreover, the high surface energy of the separated NPs after sonication due to the prevention of aggregation may cause return re-dispersion (Wassel, Grady et al. 2007). Surface coating is another strategy lead to avoid particles in colloidal assemblies.

2.8.1.1.3 Stability and reactivity of magnetic nanoparticles

MNPs can apply in WW treatment however the aggregation and agglomeration of the particles during the treatment may reduce the performance of particles. Maintaining the rapid and fast interaction between contaminants and MNPs is relying on the active site of particles. Surface modification is an approach for this objective to enhance activity and stability. A thick coating layer can influence of magnetite strength of particles, and also may impact on the reactivity of contaminants fraction with magnetic NPs. Some studies reported that the rate of reaction may reduce after surface modification of humic acids (Liu, Zhao et al. 2008). Further modification also by modification the enhancement of the number of active sites can impact on contaminant removal.

2.8.2 Graphene

Graphene is a single- layer hexagonal structural material with carbon lattice of SP^2. Because of the symmetric equivalence of two atoms in the initial unit cell, graphene illustrates dispersion energy near Fermi level (Novoselov, Geim et al. 2005). Adsorption of various heteroatom molecules such as borazine ($B_3N_3H_6$), triazine ($C_3N_3H_3$), or benzene (C_6H_6) on the graphene sheet have been investigated. As they found, molecular adsorption on graphene sites depend on the magnitude of the band gap of compound adsorbed (Novoselov, Geim et al. 2005). The adsorption of 12 kinds of metal adatoms was investigated based on stable hybridization between adatom and electronic state of graphene(Chan, Neaton et al. 2008).

2.8.2.1 Graphene oxide

The application development of nanotechnology for the treatment of WW is sped up (Mauter and Elimelech 2008). Graphene and its derivate especially graphene oxide (GO) was investigated due to the active functional groups for adsorption of materials. The three-dimensional constructors of GO permit to interlink with another functional groups through layers of the GO. The particular presence of oxygen in some functional groups such as epoxy could be the driving force to start other chemical reactions (He, Klinowski et al. 1998). Figure 3-6 shows the schematic structural of GO as a model.

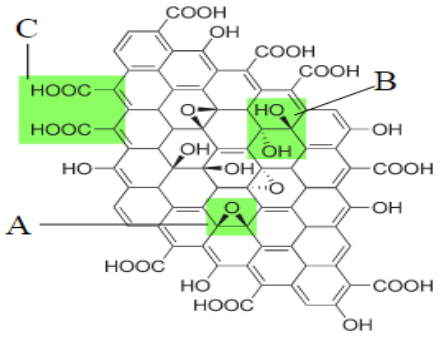

Figure 2-6 A new structural model for graphite oxide(He, Klinowski et al. 1998)A, B, and C demonstrate some active sites for interaction

GO has a tremendous absorption capacity for some of the contaminant such as methylene blue (MB) (Yang, Chen et al. 2011). The maximum absorption capacity of GO is 714 mg/g. While the initial MB concentration is lower than 259mg/L, the removal efficiency is higher than 99%, and almost the solution decolorized after the explosion with GO. Apparently, the regulation of GO efficiency is influenced by temperature, pH, ionic strength, and concentration of initial MB in solution. Due to the unique properties of graphene oxide, it had been used as sorbent some heavy metals; such as Cd (II) and Co (II) from the huge aqueous solution. Also other factors like pH and temperature can impact on the efficiency of GO for their removing. The maximum capacity of sorption had reported on GO sheet at pH 6.0±0.1 and T=303 K, 106.3 and 68.2 mg/g for Cd

and Co ions respectively (Zhao, Li et al. 2011). Schematic trapping the heavy metals by GO displays in Figure 2-7.

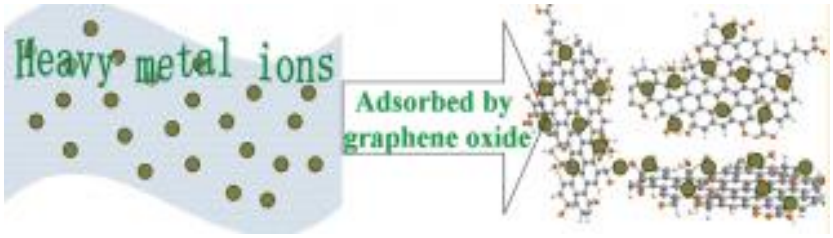

Figure 2-7 Heavy metal adsorption by GO sheets (Zhao, Li et al. 2011)

Another research has been done on the removal of tetracycline's antibiotics from the aquatic environment by (Gao, Li et al. 2012). Contaminated WW with pharmaceutical antibiotics is an important concerning for environment. Their residue may remain in surface water, soil, or even through drinking water by groundwater (Ji, Chen et al. 2009). Table 2 demonstrates the capability of the GO for eliminating the toxic elements from water milieu. For instance, tetracycline due to its structure has affinity to deposit on GO via π-π interaction and cation–π bonding. GO illustrates 313 mg/g for maximum adsorption capacity by Langmuir and Temkin model (Gao, Li et al.2012).

Table 2 Adsorption competence of graphene oxide for removing the pollutant from WW.

Adsorbent	Pollutant	Ref.
Ultrafiltration membrane with GO	Remove hydrophilic particles in WW	(Ji, Chen et al. 2009, Lee, Chae et al. 2013)
GO and TiO_2	Removal Cr(VI) from water	(Gu, Wang et al. 2013)
GO	Impact on microbial community	(Ahmed and Rodrigues 2013)
Polyethersulphone unwrapped GO	Remove Methylene blue and cationic dye	(Zhang, O'Hara et al. 2013)

Magnetic graphene oxide(MGO)	Remove Cr(III)	(Deng, Zhang et al. 2013)
SPIONs and GO	Arsenic removal	(Chandra, Park et al. 2010)
GO and magnetite composite	Methylene blue from aqueous solution	(Ai, Zhang et al. 2011)

2.9 Adsorption study

Depend upon the nature force of adsorbate to attach with adsorbent, may classified adsorption into two main groups:

Physical adsorption (physisorption):

If the attraction force between the adsorbate and adsorbent confines to Van der Waals forces, the adsorption is called physical adsorption. It would be reversible and usually take place in low temperature, therefore by increasing the temperature the capacity of the physisorption decreases. Changing in temperature can made changes on the adsorption attachment.

Chemical adsorption (chemisorption):

The attraction force between the adsorbate and adsorbent are an almost chemical bond, frequently elevating the temperature induces evaluation more interaction between chemical bonds. This kind of adsorption identifies as Langmuir adsorption. The interaction force between particle and surface is quite definite and irreversible easily.

In continue we explain about the physical isotherm Freundlich adsorption equation as a known definition for adsorption;

This equation was expressed for the first time by Freundlich in 1909, by his definition; the amount of adsorption of a gas on a solid surface rely on pressure and a constant of the equation.

He defines the adsorption as below equation

$$\frac{x}{m} = K(p)\text{^}\frac{1}{n}$$

Where x is the mass of gas adsorbed on the mass of m solid adsorbent at p equilibrium pressure or sometimes place c instead of that to demonstrate equilibrium concentration of adsorbate in solution and constant k. This equation experimentally useful before the pressure variation reaches saturated pressure.

2.9.1 What is the Adsorption Isotherm?

The process in which adsorbate adsorbed on the surface of the adsorbent at a constant temperature is adsorption isotherm.

Adsorbate + Adsorbent ===== Adsorption

A+B====AB

Adsorption isotherm theory is described by various models; Freundlich, Langmuir, and BET. According to the adsorption equilibrium principal, adsorption proceeds in direct of equilibrium for the curve of adsorption and pressure. The number of adsorbate decrease by adsorption on adsorbent along with an increase the pressure toward saturation pressure point. After that, no more adsorption will occur.

CHAPTER 3: EXPERIMENTAL SECTION

Briefly, we attempted to synthesize some NPs including iron oxide as an inert and non-toxic composite for eliminating the nanoscale contaminants from water and thus manipulate gathered NPs by exterior laboratory magnet. To reach this objective, two kinds of nano hybrids composed of iron oxide and polyethylene glycol (PEG) (20000 Da) were synthesised for the first which is nano hybrid, and for the second one which is composed of iron oxide, PEG and GO. Then the samples were exposed to these NPs and removed by an exterior magnet. The changes of samples before and after treatment were explored by means of various analytical methods such as FT-IR, UV-vis, DLS, AFM and TEM. The samples after exposure to SPION/GO@PEG shows contaminants adsorption such as previous one but some portion of GO was separated from nanocomposites and remains in wastewater after treatment. Attendance of GO in water causes some changes in cluster distribution size and shape of remained particles in wastewater after treatment.

3.1 Materials

WW sample from glycerine and sugar (as simple natural HTC samples) that received from Tier University in Germany. The samples were produced by HTC process with followed information; 150 g sugar (normal household sugar)/ 150 g glycerine dissolved in 1.5 L water while 100 ml H_2SO_4 was added as catalyst. The reaction continued in 180^{o} C and pressure of 20 bar for 180 minutes. The composition measurements of HTC waste water of sugar and glycerine are as below.

Measurements	Sugar	Glycerin
Chemical oxygen demand total (mg/l)	23295	23575

Chemical oxygen demand dissolved (mg/l)	23080	22780
Total organic carbon (TOC) (mg/l)	8350	8560
Dissolve organic carbon (DOC)(mg/l)	8520	8670
pH	3.9	4.0
Conductivity (ms/cm)	10.5	10.4

Ferrous chloride tetrahydrate by Sigma Chemical co., ferric chloride hexahydrate from Frisher scientific co., and hydrochloric acid A.C.S reagent 37% were used. Hydroxide ammonium solution and poly ethylen glycol(PEG) (20000 Da) were also supplied by Sigma Aldrich co. for synthesized the SPIONs. GO was provided by modified graphene sheet to graphene oxide (GO) powder which was obtained from Morugun; the procedure of synthesis is in his article. The water throughout this work was the distilled water and deoxygenated Milli-Q ultrapure water grade reagents produced by Millipore Milli-Q Gradient A10 (ZMQS6V0T Ultra-pure Water Purifier) without further purification.

Equation below gives the chemical reaction of Fe_3O_4 precipitation (1)

$$Fe^{+3} + 2Fe^{+2} + 8\ NH_4OH \longrightarrow Fe_3O_4 + 4\ H_2O \qquad (1)$$

Two different MNPs substrates were used for treatment, for providing appropirate hybrid NPs, we performed as following; First adsorbate candidate was prepared by synthesizing of SPIONs with high polymeric molecular weight of PEG (20000 Da) as coating layer. For the second nanocomposite we generated MNPs congregated with GO and PEG (20000 Da) as oxygenated and other remady supporter layer to improve adsorption properties for decontamination. The NPs well-done synthesized by co-precipitation method.

3.2 Synthesis of SPIONs @ PEG

The NPs were synthesized with some modification as follow Molina's article (Molina, et al. 2013). Briefly, 1.0 mL of $FeCl_2.4H_2O$ (0.199gr) and 4.0 mL of $FeCl_3.6H_2O$ (o.540 gr) by respect of molar ratios (2:1) prepared in 1M solution of HCl were mixed gradually to ambient temperature and stirred under nitrogen gas to prevent excess oxidation and lose the desire structure and properties. Then for precipitate, the mixture was added by syringe to the volume of 50 ml of NH_4OH (0.7M) as a precipitate agent. Then for complete the reaction, let enough time around 15 min in stirring condition. At this stage, the solution was centrifuged, and the precipitate was decanted. Then washed one time with Milli-Q water and repeated decantation by centrifuging. Next step followed by the addition of a 5mL solution of PEG 20000 Da (5%) for coating the bare NPs. This mixture was left stirring for 20 min. The solution was centrifuged several times by washing with distilled water, acetone, and ethanol. The new precipitate lead to covered NPs with PEG was gathered and let it dry in room temperature.

3.3 Synthesis of SPIONs/GO@PEG

3.3.1 Synthesis of Graphene oxide from graphite powder (Following some modification Hummer method)

In brief, Graphite powder (2gr) were stirred in 98% H_2SO_4 (45ml) for 2 hours. The sufficient amount of $KMnO_4$ was gradually added to the above solution by holding the temperature below the 20 °C. Then increasing the temperature until 35 °C and stirring the mixture for 2 hours. The resulting solution was diluted by adding 90 ml of distilled water under vigorous stirring. The suspension was further treated by adding 10 ml H_2O_2 (30%) solution and 150 ml of distilled water. The suspension graphite oxide was repeatedly centrifuged while washing with first 5% HCl aqueous solution and second by distilled water until the pH of the solution become neutral. The resulted GO nanosheets were precipitated by adding 160 ml of distilled water then were

irritated by ultrasound sonication for 1 hour to exfoliation of the graphitic oxide into a GO monolayer (Krishnamoorthy, Veerapandian et al. 2013).

3.3.2 Fabricated second hybrid nanoparticle SPIONs/GO@PEG

For achieving NPs of iron oxide with GO with PEG coating, the procedure was done as follows; $FeCl_2.4H_2O$ (2.0mL, 0.199gr) and $FeCl_3.6H_2O$ (4.0mL, 0.54 gr) with molar ratio of (1:2) were prepared in HCl solution (1M). These two different chloride iron were mixed each other drop by drop with nitrogen gas in room temperature string. 25 mg GO was added to the solution of NH_4OH (50mL, 0.7 M) to solve. The primary solution placed in ultrasonic condition for dispersion and solving around 30 min. Then, Iron solution was added by syringe under nitrogen gas to the hydroxide ammonium solution step by step to obey co-precipitation condition. During this combination, formation of NPs at the bottle was observed. Taking 15 min stirring in the stage to certify for completing the reaction. The mixture was decanted with distilled water several times to remove unreacted GO and neutralized the solution. Then for covering with PEG, provided (25mL, 1%) PEG (20000 Da) was mixed to the suspended NPs while stirring overnight. Next procedures were done as before for dialysis. All precipitated NPs in water dried by freeze drying apparatus for more than three days to obtain dried NPs.

3.4 Characterization

The prepared magnetite iron oxide nanoparticle were characterized using some techniques for measurement. The size, shape, and surface topography of NPs were characterized by Atomic Force Microscopy (AFM) (Atomic Force Microscope, Bruker/ Santa Barbara, CA). The AFM images were obtained in the air at room temperature using peak force tapping mode. During tapping mode the cantilever is driven to oscillate up and down to prevent the tip stick to the surface of samples but it comes close to the surface. All the scan except of sugar HTC untreated sample were performed at the rate of 1Hz using etched silicon cantilevers (ACTA from

AppNano). For AFM analysis, 10 µl of each sample was diluted by distilled water depositing onto cleaved sheets of mica surface, the surface was air-dried in the dust-free enclosure. The images were made in Tapping model Etched Silicon Probe (TESP) with the spring constant of ≈ 42 N/m and tip radius of < 10 nm. Nanoscope Image Analysis software examined all the images and followed by section analysis and measurement of the height and diameter. The TEM images were taken by (TEM, Model JEM 2100F-JEOL Company) in combination with EDC. The TEM was operated at 200kV energy for acquiring enough bright field for sample images.

Prior to the microscopic analysis, NPs were put 10 min in a sonication bath for reasonable dispersion. SPIONs intend to accumulate for constitution the bigger particle as the reason of the tiny size of the NPs and high active potential surface. Fourier Transform Infrared Spectroscopy (FT-IR) (IR-ATR-Bruker) measured our samples in solid state at room temperature for illustration functional groups by IR spectra. Density and diameter of particles might be probed by Diffraction Light Scattering (DLS).

WW samples were provided by HTC process of Germany. The pH of samples without any modification through treatment were four afterwards the regular process. They were characterized by the same technique, for FT-IR spectroscopy, DLS, and AFM analysis. The real samples were vaporized before the sampling for infrared then the dried sample transferred to the KBr crystal for absorption measurement. The samples were identified presence functional groups and chemical bonding of the dissolved material in the water. The water spectra peaks in WW samples cover the real spectra of involved sample.

WW samples were analyzed by Ultra Vision spectroscopy (UV) (Varian Cary 100 Bio UV Visible Spectroscopy); the modification of maximum and condition of spectra before and after treatment can lead the evaluation the effectiveness of this strategy. Diffraction Light Scattering (DLS) (Zetasizer model ZS) technique allows the determination of the size distribution profile of particles in suspension based on Rayleigh scattering with respect to Brownian motion. Hence the density of the scattered light represent the circumstance of aggregated or agglomerated of nanoparticle in the liquid. This technique also can certify the results by comparing differentiate of samples status after treatment. Removal percent and adsorption amount of SPIONs would be calculated by the reduction in density of contaminants particles in water after the treatment process.

CHAPTER 4: RESULT AND DISCUSSION

4.1 Structural Properties of SPIONs

4.1.1 The FT-IR spectra of SPIONs@ PEG

Fourier transform infrared absorption spectra were collected in the IR range from 4000 to 500 cm^{-1} using Bruker spectrometer in attenuated total reflectance (ATR) mode. The beam was polarized pass the sample on the high throughput KBr ATR crystal. The powder sample of SPIONs was analyzed by this equipment for proof dominant functional groups. The FT-IR spectra of the synthesized sample, SPIONs@PEG content, is shown in Figure 4-1. In this spectra, the broad bond at 3400 cm^{-1} attributed to the stretching vibration of the O-H groups in PEG. The peak at 1670 cm^{-1} corresponds to the stretching vibration of C=O of carbonyl and carboxyl groups. The peak at 570 cm^{-1} and 400 cm^{-1} are desscribed to the Fe-O-Fe stretch bind that split into two. The identified peaks provide evidence for iron oxide representation by strong stretching and bending vibration in the region between 400 to 600 cm^{-1} with shoulders and definite split for assigning the Fe-O.

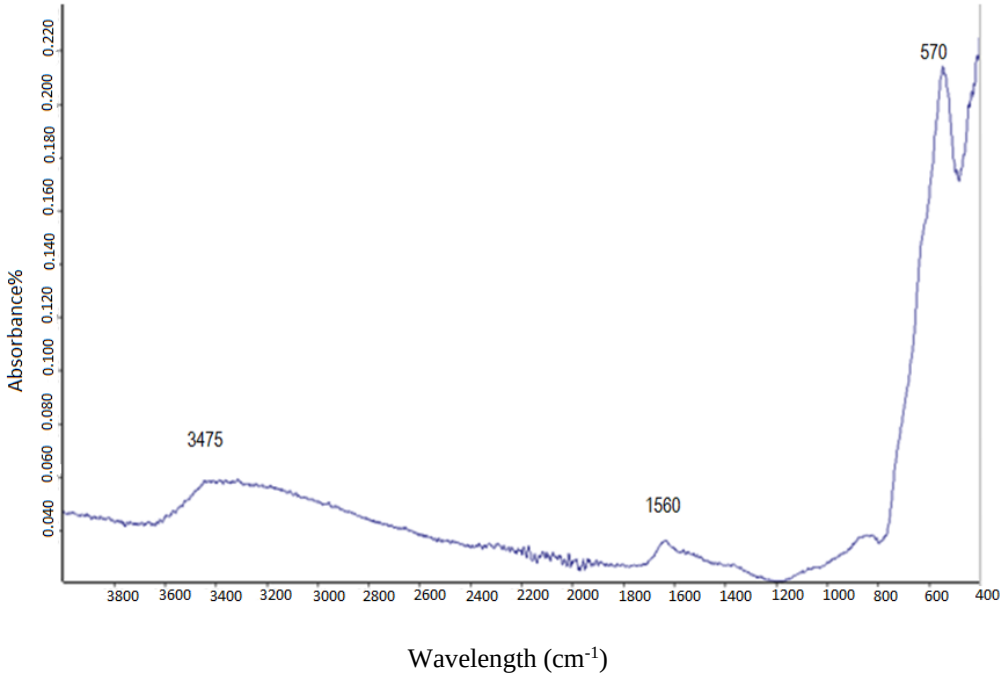

Figure 4-1 FT-IR spectroscopy of SPION@ PEG

4.1.2 The FT-IR spectra of SPIONs/GO@PEG

The spectrum of the sample SPIONs/GO@PEG is characterized by the widening of the upper 3000 cm $^{-1}$ is pronounced by stretching the vibration of hydroxide and carboxylic groups in PEG and GO. As it shows in Figure 4-2, the widening demonstrates some further peaks of oxygen content which may overlap with main adsorption based on OH and OOH. These groups intend to present the adsorption in high wavelength as it is observed in spectrum. The stretching vibration bonds of C-H of the PEG is found at 2885 and 2830cm^{-1}. The peak in 1450 cm^{-1}shows C-O stretching vibration, more over in this region other peaks can pronounce the O-H bending vibration around 1100 cm^{-1}. Carboxylic functional groups in GO appear strongly in 1570cm^{-1}. Other less pronounced peaks such as bending vibration of C-H groups in 1450 cm^{-1} can be observed. In the comparison between the two spectra of SPIONs@PEG and SPIONs/GO@PEG composites, almost all of the absorption peaks of primary functional group of GO, PEG and SPIONs also appear in the spectra with a slight shift of position and intensity. By further analysing the absorption area higher than 2800 cm^{-1} , we can confirm the attendance of various

functional groups including oxygen. It is probable due to the overlap of the hydroxid group widening in PEG and GO. Therefore, it may suggest the presence of some hydrogen bonding between oxygen content functional groups. These results confirm the presence of PEG as a coating of SPIONs, in agreement with Wang et al. report (Wang, Feng et al. 2012). As the schematic illustration shows there are further interactions between OH functional groups of PEG and various functional groups in GO.

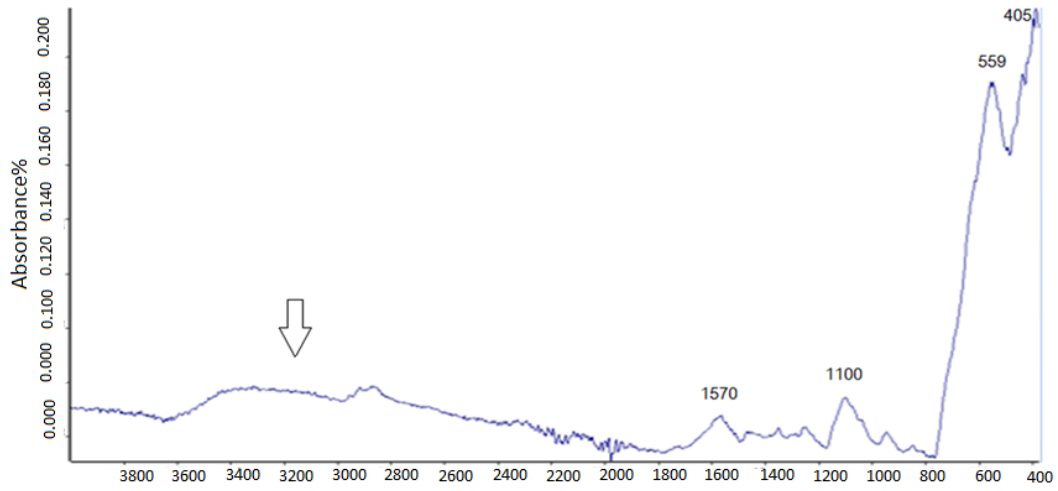

Figure 4-2 FT_IR absorbance of SPION/GO@ PEG

4.1.3 AFM analysis of SPION@ PEG

The size and surface topography of Fe_3O_4 NPs in SPIONs@ PEG NC were analyzed by AFM. This technique is providing information with spatial resolution. AFM images of SPIONs @ PEG presented in Figure 4-3 by indicating arrow signs. All the light blue spots where 12 points were selected, are in cluster form as observed in Figure 4-3(b). The altered shape and size of NPs represent aggregation in spite of sonification before analysis, whereas the drying process performed in air condition prior to taking the images, significant parts of the nanoparticle intended to transform into cluster form instead of separated nanoparticle. The bright spot provides the estimation of smaller cluster height of 1.536 nm and means diameter approximately 40.58 in Figure 4-3 (b). The results show that the size and morphology and even the density were

different. Since the particles make biger cluster shape the revealed density of each group seems as the substitute of each nanoparticle.

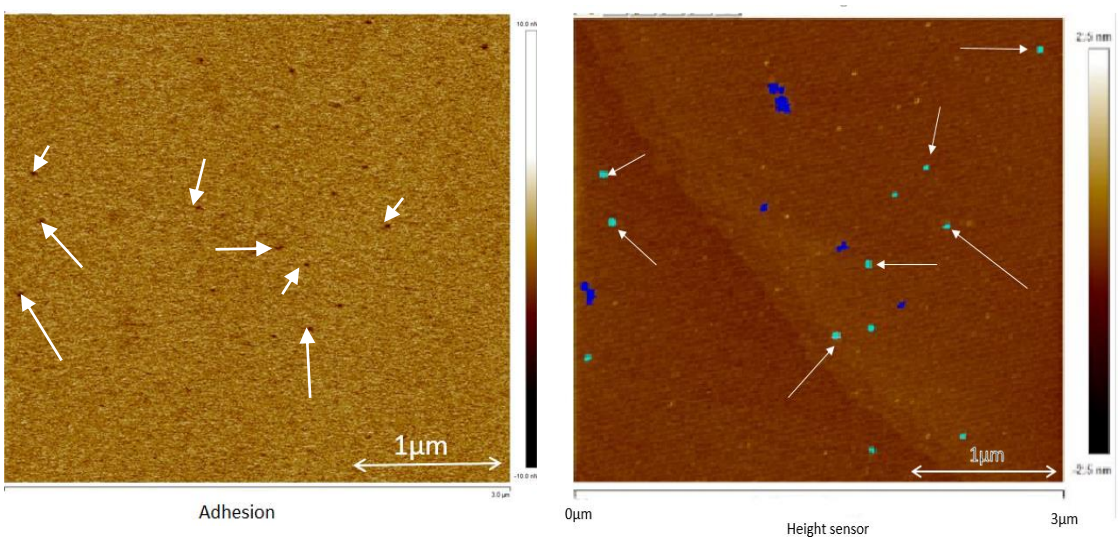

(a) (b)

Figure 4-3 (a) AFM image of NPs constitute of SPIONs @PEG (b) AFM image of SPIONs@ PEG NPs for statistical measurement by the light blue spots defined

Table 3 SPIONs @ PEG AFM details of Figure 4-3 (light blue spots) image

Parameter	Mean	Minimum	Maximum	Sigma
Total Count	12.000	12.000	12.000	0.000
Density	1.333(/µm^2)	1.333(/µm^2)	1.333(/µm^2)	0.000(/µm^2)
Height	1.536(nm)	0.976(nm)	2.086(nm)	0.318(nm)
Area	1313.210(nm^2)	892.639(nm^2)	1888.275(nm^2)	318.423(nm^2)
Diameter	40.583(nm)	33.713(nm)	49.033(nm)	5.001(nm)

4.1.4 AFM analysis of SPIONs/GO@PEG

The AFM image of the second synthesized NPs, SPIONs/GO @PEG is shown in Figure 4-4 matches well with the AFM image of graphene (Fan, Peng et al. 2008). The AFM represents the plaque shape which fully exfoliats the graphene oxide sheets (Stankovich, Dikin et al. 2007) as reported before. As mentioned in the last report (Stankovich, Dikin et al. 2007) The average height was larger than 1.3 nm. The GO sheet is attached to the SPIONs and fully covers the nanoparticle as seen in Li studies (Li, Cao et al. 2011). The image demonstrates the lower density in comparison with the previous NPs. As illustrated in the picture, the large aggregate clusters of NPs are visible but are not suitable for accurate measurement.

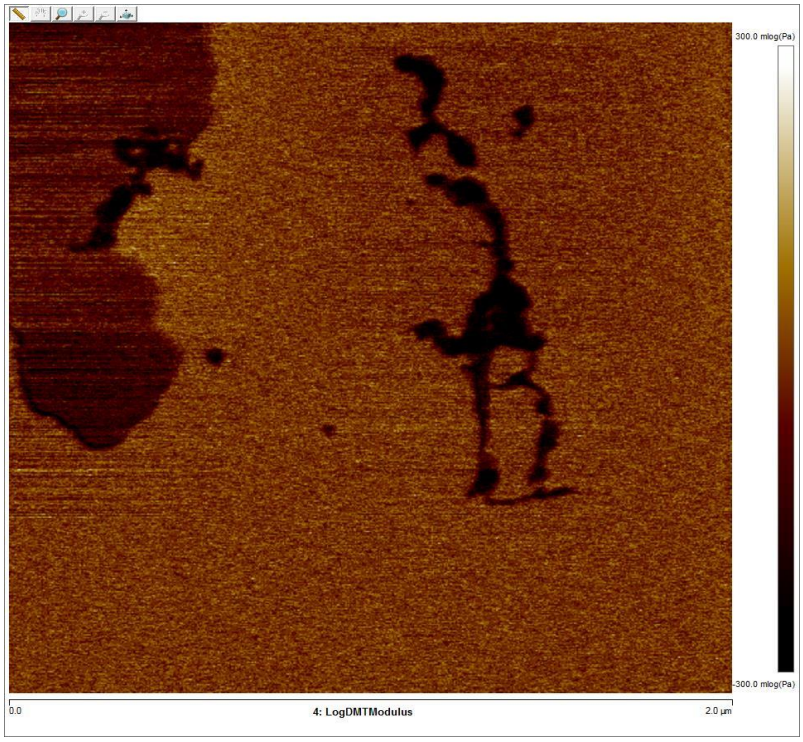

Figure 4-4 AFM image of amorphous shape plaques of nanocomposite include SPIONs / GO @ PEG in aggregated form

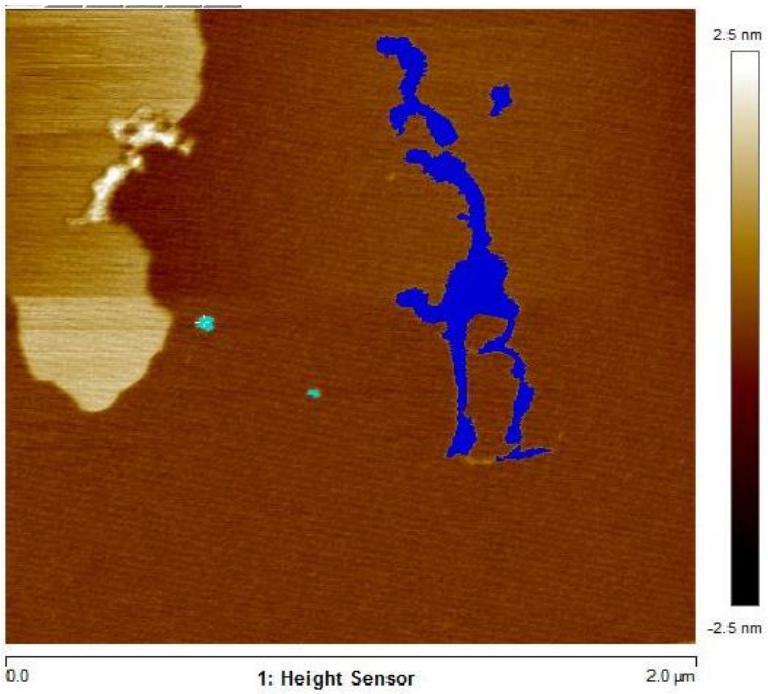

Figure 4-5 Tapping mode AFM image of SPIONs/GO @PEG

Table 4 Detail information of NCs of SPIONs/GO@ PEG by selection of two light blue color point in low agglomerated shape of Figure 5-5

Parameter	Mean	Minimum	Maximum	Sigma
Total count	2.000	2.000	2.000	2.000
Density	0.500(/µm^2)	0.500(/µm^2)	0.500(/µm^2)	0.000(/µm^2)
Height	1.307(nm)	0.823(nm)	1.791(nm)	0.484(nm)
Area	1144.409(nm^2)	595.093(nm^2)	1693.726(nm^2)	549.316(nm^2)
Diameter	36.982(nm)	27.526(nm)	46.438(nm)	9.456(nm)

The above data represent the two bright blue spots with the lower aggregation. Other sections show massive cluster formation in which obtaining detailed morphology were not measurable. The diameter of the nanocomposite from SPION and GO shows less size distribution than the previous SPIONs. Such aggregation is supposed to arise from the strong interaction between

functional groups in GO, which they prevent further aggregation and agglomeration of SPIONs individually. However the diameter size is close to SPIONs@ PEG cluster, the presence of GO could be a rational reason for this diameter distribution.

4.1.5 TEM images of NCs involve SPIONs@ PEG

The fine crystalized SPIONs@ PEG in nanostructure range of size and morphology is demonstrated by the TEM. Related images MNPs shown in Figure 4-6 are similar to the TEM images of SPIONs in the research results of Schear et al. (Schaer, Crittin et al. 2014) who evaluated the size distribution around 10 nm for the PEGylated SPIONs (Herve, Douziech-Eyrolles et al. 2008) with co-precipitation method preparation. As it shown in the Figure 4-6b, the corresponding NP constitute the cluster shape due to high active surface site and the fine, thin layer of PEG.

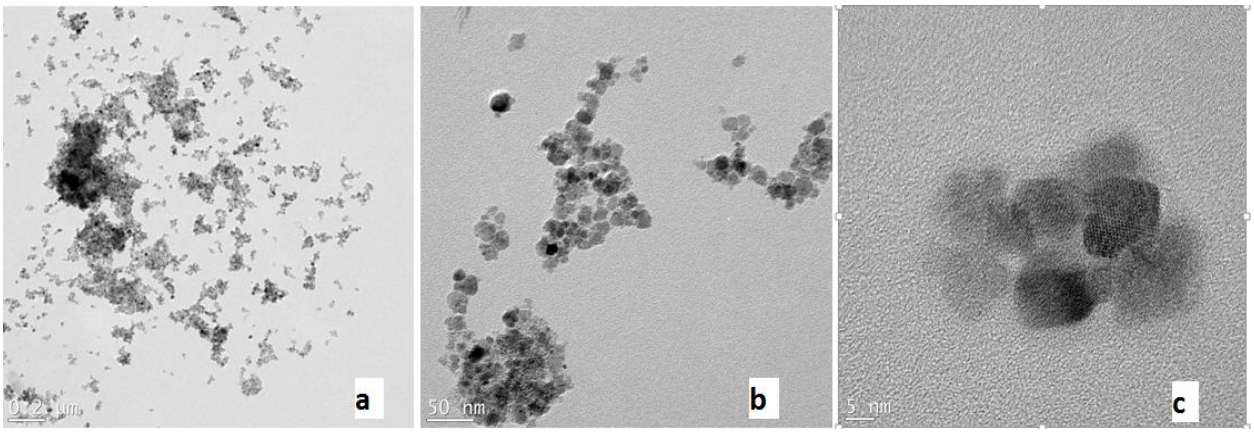

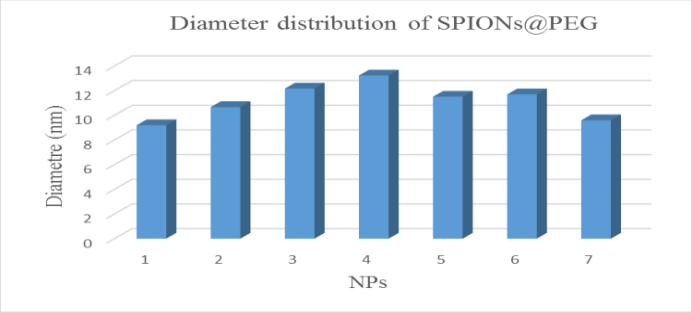

(d)

Figure 4-6 TEM images of NCs (SPIONs@ PEG) in various scale (a-c)

(d) Histogram of SPIONs@ PEG NPs in respect of diameter size (nm)

By the histogram of the MNPs the average size of the NPs, (11nm) can be found, although the PEG layer is not observable seprately, it can also be compared with the previously mentioned articles for proof.

4.1.6 TEM images of MNPs of (SPIONs/GO@PEG)

The morphology and structure of the hybrid composite (SPIONs/GO@PEG) were thoroughly analyzed by TEM observation. Figure 4-7(a-c) evaluates the diameter size of NPs including the crystalline and amorphous shapes shown by the high-resolution TEM images. The images confirm the colloid configuration that induce the size estimation just as determined with small aggregation groups such as mentioned in the previous reports (Fan, Peng et al. 2008, Laurent, Forge et al. 2008). The average size of isolated NPs was 11.8 nm as it measured by histogram Figure 4-7 d.

The Fe_3O_4 particle wrapped with GO sheets, which can control the agglomeration of the magnetic iron oxide and help to have a good dispersion in comparison to the absence of these NPs. The TEM images indicate that the GO is well-attached to the SPIONs and has not remained isolated.

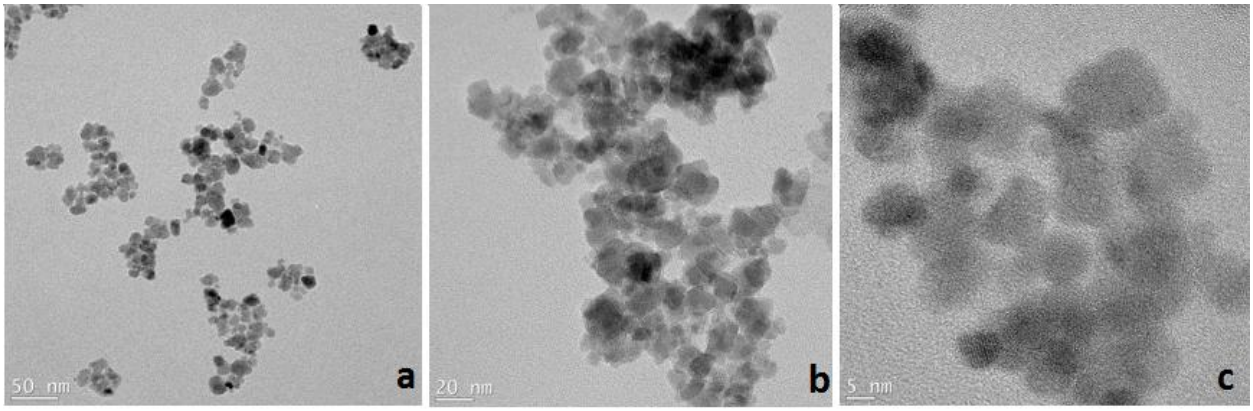

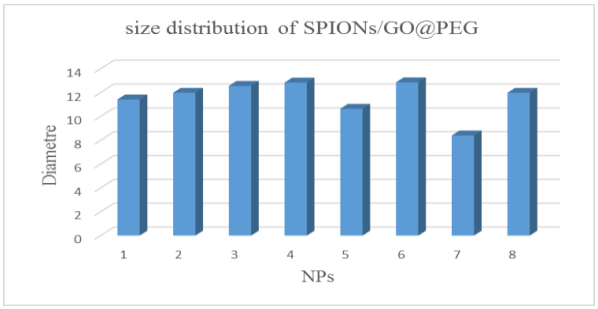

(d)

Figure 4-7 TEM images of SPIONs/GO@ PEG hybrid composite (a-c) and (d) TEM histogram column chart for pertained NPs for diameter size evaluation

The obtained images from TEM are comparable with the picture from the hybrid composite of Fe_3O_4/GO (Yang, Zhang et al. 2009). Considering this point that the GO with the various functional groups has the linkage potential between oxygen and carbon groups may promote the affinity of the component for rearrangement. The GO sheets have coordination interaction with hydroxyl, carboxylic and epoxy groups at the edge of graphene (Yang, Zhang et al. 2009). The configuration mode of place ment of each particle can impact on shape and size of the cluster to boost the stability.

4.1.7 DLS analysis of (SPIONs @ PEG)

Dynamic light scattering curve revealed the dispersion of associated MNPs concludes SPION @ PEG in an aqueous medium in room temperature Figure 4-8.The principal peak for qualifying

the distribution of NPs in distilled water in Figure 4-8 shows 400- 548.8 nm for this nanoparticle. The determined intensity percentage for these NPs is 43%, and polydispersity index (PDI) is 0.628. The measured Z-Average is 1189 (nm) in room temperature analysis. It is assumed, the reasons of aggregation configuration can be for the thin layer of PEG coating, and the weak influence of hydrocarbon groups induce no strong barrier layer for high agglomeration affinity. This rational approach states due to van der Waals force and magnetic dipole-dipole interaction between the super active MNPs notably with the determined diameter this agglomerated configuration justified.

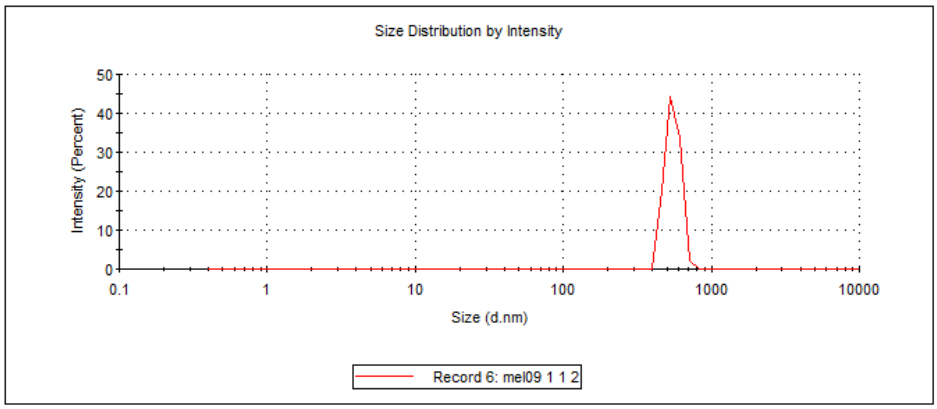

Figure 4-8 Illustrate DLS analysis curve of SPION@PEG NPs which aggregated into cluster

The colloidal form stability of the MNPs in acidic medium may provide positive groups on the surface of SPIONs for electrostatic repulsion, this can exhibit less aggregation (Gautier, Munnier et al. 2012). In this case due to the neutral acidic environment the MNPs will aggregate extraordinary as it emerges in SPIONs@ PEG.

4.1.8 DLS analysis of (SPION/GO@ PEG)

By DLS measurement, the mean hydrodynamic diameter for aggregation cluster of MNPs was obtained to be 150-242.5 nm with a polydispersity index (PDI) of 0.512. This analysis in Figure 4-9 illustrates only one population with the highest intensity of 38%. As it can be observed in the size distribution by concentration curve, the SPIONs@ PEG accumulates in aggregated form with 548.3 (nm) in Z-average. It demonstrates the SPIONs in spite of attendant the polyethylene

glycol in high polymeric molecular weight intend to stabilize by agglomeration and aggregation form. Naturally this configuration for SPIONs is anticipated. This unique distribution colloidal shape that is illustrated by DLS emphasizes the new interaction between these MNPs. By comparing the significant distributions, diameter sizes differentiate of SPION @PEG and SPIONs/GO@PEG can be explained the distribution diameter can be reduced in SPION/GO @PEG due to the presence of the GO accompanied with SPIONs. GO for possessing various functional groups make steric hindrance for further agglomeration form. Therefore, the resulted particle mass for SPIONs/GO@ PEG is considerably lower than SPION @PEG. In SPION @PEG case, the intensity percentage, diameter size and also polydispersion parameter are much more than SPIONs/GO@PEG NPs. Moreover, they reduce aggregation form by a steric effect of engaging free active site of SPIONs and GO for further interaction. The scattering light intensity shows quadratic dependence on the volume of scattering according to the classical Rayleigh theory (Sipos, Berkesi et al. 2003). Based on Rayleigh theory elastic scattering of light or electromagnetic radiation by particle contact which are smaller than wavelength of light induces this scattering and polarizability of the particles. In general, the larger molecule contributions intend to monodispersity compared to polydispersity.

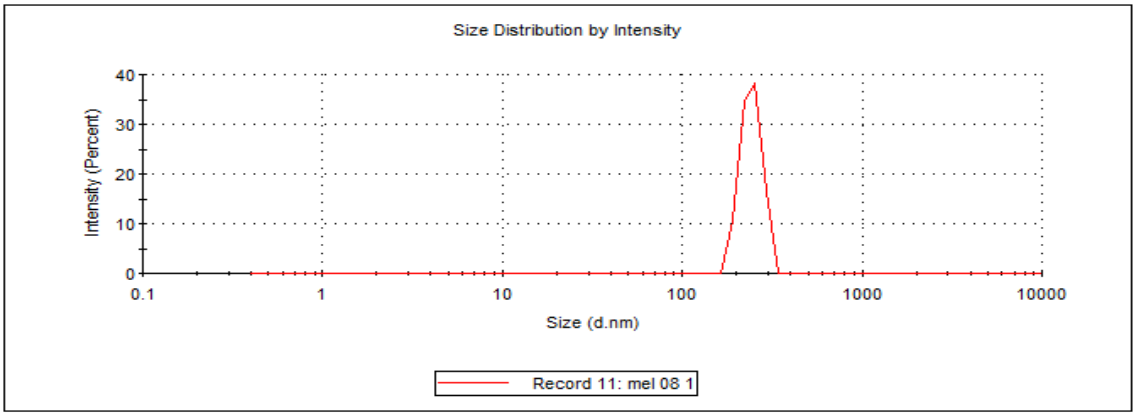

Figure 4-9 DLS analysis Curve of SPION/GO @ PEG

4.2 Wastewater treatment by synthesized NPs

The most experimental goal conducted by exposure of synthesized NPs to our objective samples from glycerine, and sugar. Bach reduction contamination experiments were conducted by adding

the 10 mg MNPs to 10 ml of the samples solution with PH = 4 after HTC, in the sample tube. By this approach, After a few seconds of shaking for sufficient contact time, the appropriate dispersion in samples solutions took thirty minutes to remain in the steady state in order to precipitate all contaminated particle that accumulate with magnetic NPs. One handle magnet in the laboratory could conduct MNPs and pollution fraction to the corner of the sample tube for removal.

In Figure 4-10 sugar and glycerine WW by application of MNPs (SPIONs@ PEG) as the strategy for reduction of contaminants nanoparticles were carried out.

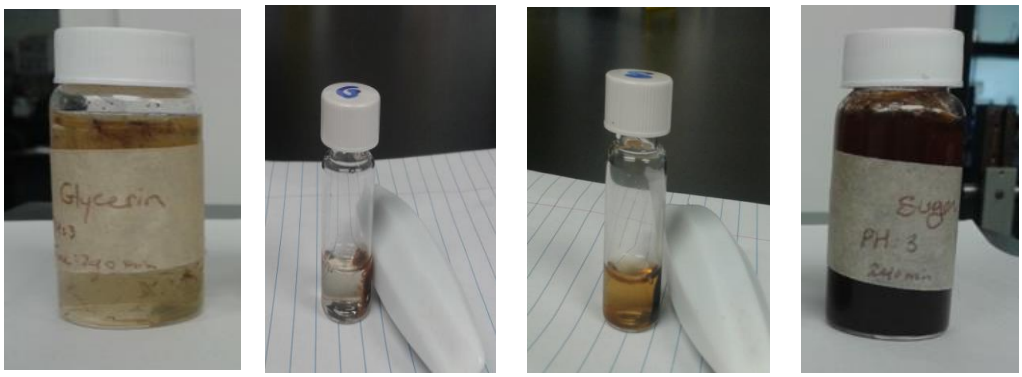

(a) (b) (c) (d)

Figure 4-10 (a) Glycerin sample generated by HTC; (b) Glycerin sample after treatment by SPIONs@ PEG; (c) Sugar sample after SPIONs @PEG exposure; (d) Sugar sample via HTC

After exposure the samples to the (SPIONs/GO@PEG) for partial nanocontaminants removal, some part of GO separated from MNPs and remain in the samples after treatment. Therefore this GO attendance in liquid samples make some variation for performed analysis. The color of the samples after take out the collection of MNPs and nanocontaminants also illustrated the presence of GO in wastewater samples after treated.

4.2.1 UV-vis Spectroscopy of Glycerine

The contaminated samples were analyzed by UV absorption spectroscopy. Prior to carrying out the spectra preparation, the sample to 25% initial concentration was done. The adsorption range

between 0 to 6nm for glycerine and 0 to 10 nm for sugar was chosen between the wavelengths of 200 to 800 nm.

Figure 4-11 shows the UV-vis spectra of the aqueous glycerine WW via HTC before any treatment process. The spectrum of water generally expected between 280-300 nm (Knubovets, Osterhout et al. 1999) for water at pH around 3-4. The adsorption spectra of WW of glycerine do not show any max peak in this area while the adsorption peak of waste solution exhibited obvious ranges between 200-280 nm. The UV spectra of glycerine WW after treatment by magnetic NP demonstrated the lower density of adsorption. Meanwhile, the wavelength area shows no difference. The organic compound particular, those with a high conjugation degree may have significant absorption as it is observed in this sample.

Comparing UV spectroscopy of glycerine WW before and after treatment with SPIONs@ PEG NPs demonstrated significant various between two samples. The absorption occurred in the range point of 200 to 300 nm for primary glycerine WW. The highest absorption peak is in 3.5 albeit changed to 2.8 after reduction contamination.

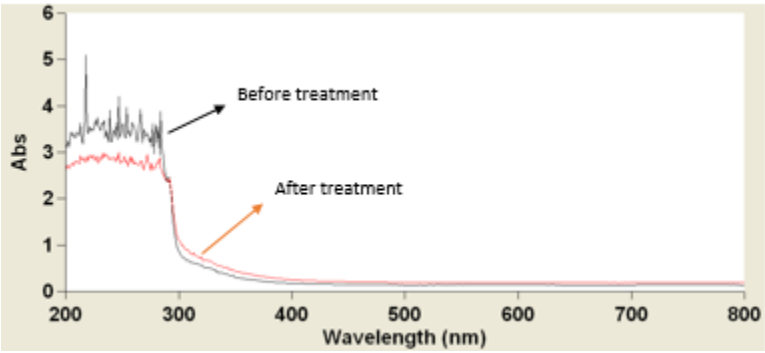

Figure 4-11 Glycerine UV-vis spectroscopy before and after treatment with SPIONs @ PEG

As mentioned before, the chemical structure as well as the color of sample solution can influence the quality and amount of absorbance in a definite area. For study on UV-vis absorption of glycerine sample after SPIONs/GO@PEG absorption reveals no significant difference between the peaks before and after treatment. Since the sample contented the GO after treatment and functional groups of that have absorption exact in this area (200-300 nm), prevention to observe reduction in absorption peaks after treatment is expected. Figure 4-12 illustrates no significant variation except of the little changes in details.

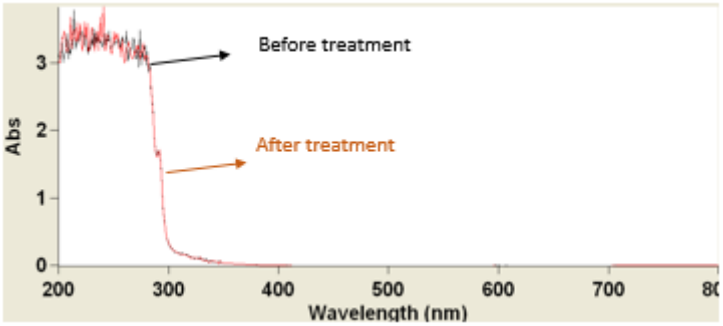

Figure 4-12 UV-vis absorption spectra of glycerine WW generated by HTC process after being treated by SPIONs/GO@PEG

4.2.2 UV-vis spectroscopy of sugar wastewater

UV-vis spectroscopy for sugar sample performed like a previous sample for dilution. The range of studying for this sample is between the range of 200-800 nm wavelength, but the absorption limitation extend somehow as the initial sugar sample peak, (0-10) for absorbance (Figure 4-13). The curve of sugar WW illustrated differentiates between the maximum range peaks and moreover the sample after treatment shows absorption under 400nm to 800nm around 0.5 in contrast mode of the untreated sample. The width of peaks located in the range of 200 – 400 with the maximum part in 200-300 nm.

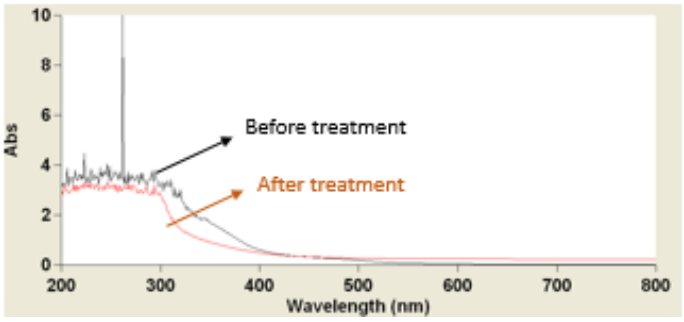

Figure 4-13 Sugar UV-vis spectroscopy analysis of sugar before and after treatment by SPIONs @PEG

The UV-vis absorption spectra of sugar WW sample via HTC original and the sample after being treated with SPION/GO@PEG is shown in Figure 4-14. A maximum absorption from original sample observed that located at 230nm, absolute sharp in high absorbance around 10. Both of

spectra peaks were in the range of 200-300 nm same as previous samples. The red color of treated sample due to the presence of GO exhibit virtual variation in quantity and quality of nanocontaminants after treatment to SPIONs/GO@PEG. Their UV spectra indicate none dominant variation between these peaks except the sharp peak of sugar WW sample.

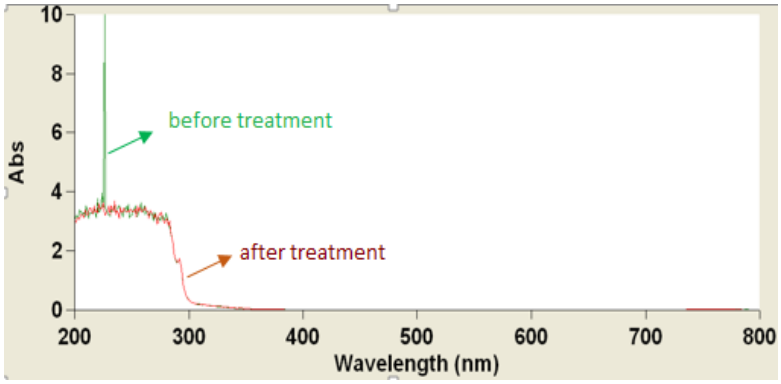

Figure 4-14 Comparison UV-vis spectroscopy curve of Sugar WW prior be treated by MNPs and the changes after exposure to SPIONs/GO@ PEG.

4.3 Analysis of wastewater

4.3.1 FT-IR spectroscopy

The FT-IR spectra of the glycerine WW sample are shown in Figure 4-15. This spectra was taken without the presence of water due to the water spectra peaks which can completely cover the materials principal peaks.

The FT-IR spectra reveal a broad peak at 3339 cm^{-1} that attribute for the widening of O-H groups. The peaks observed 2933, 2880 cm^{-1} corresponds to the OH stretching group vibration for *cis* and *trans* configuration. The peak assigned to the carbonyl stretching group at 1650 cm^{-1}. Also, there are fingerprint regions below 1100 cm^{-1}. The regions between 1450 -1100 cm^{-1} are due to O-C-H, C-C-H and C-O-H bending mode. All the spectra peak adjusted with the IR spectrum of Glycerine.

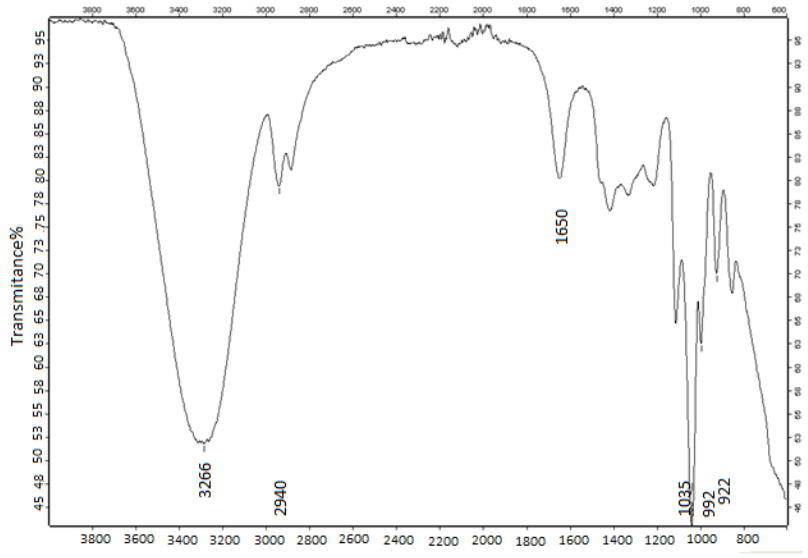

Figure 4-15 FT-IR spectrum of dried glycerine WW via HTC

FT_IR spectra of sugar WW generated by HTC with original pH =4 after implementation of HTC on original sugar feedstock obtained. The water content in the sample before analysis was evaporated to avoid any water peak overlap. As seen in Figure 4-16, OH bond widening observed at 3368 cm^{-1} strongly also confirmed that presence of OH groups in sugar structure. The sharp peaks at 1650cm^{-1} indicated the stretching vibration of the dominant C=O functional group. Also two other peaks at 1164, 1205 cm^{-1} may present the C-O bond in this spectra. Thus, it can be suggested this spectrum also confirm the presence of the primary substrate after the HTC process.

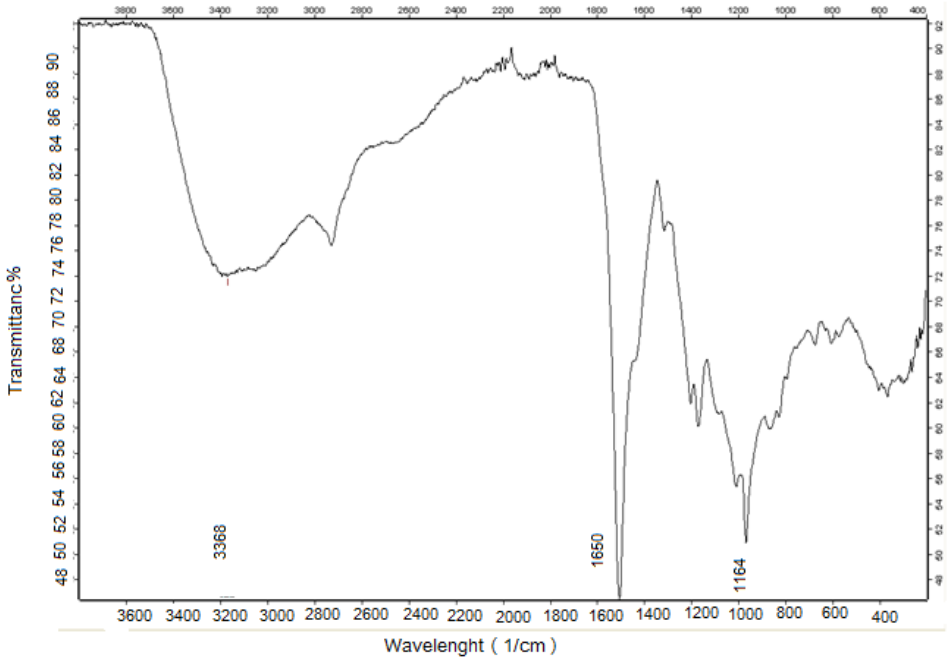

Figure 4-16 FT-IR spectra of sugar WW from HTC process

4.3.2 Dynamic Light Scattering analysis (DLS)

The main reason for applying DLS technique was to determine the size and diameter of the particle in the WW product after HTC. This method can reveal the distribution of fraction and qualifying the organization of them in liquid. Since the light in this method is coherent and monochromic, observation of the intensity of the particle is feasible. This note should be considered, this technique is based on the motion and fluctuation of the particles with a change of time.

The characterization of the WW, glycerine, and sugar, were performed using dynamic light scattering (DLS) with Zetasizer model ZS instrument.

4.3.2.1 DLS of glycerine wastewater

The resulted of glycerine WW via HTC for investigation; the particles distribution was analyzed by DLS instrument. As shown in Figure 4-17 the determined diameter distribution for glycerine WW NPs is 281.8 nm in constant temperature condition 25 °C. From the obtained result, these particles have 1.000 polydispersity index (PDI) with Z-average of 2161 (nm). The intensity of the NPs is about 67% with these size distribution.

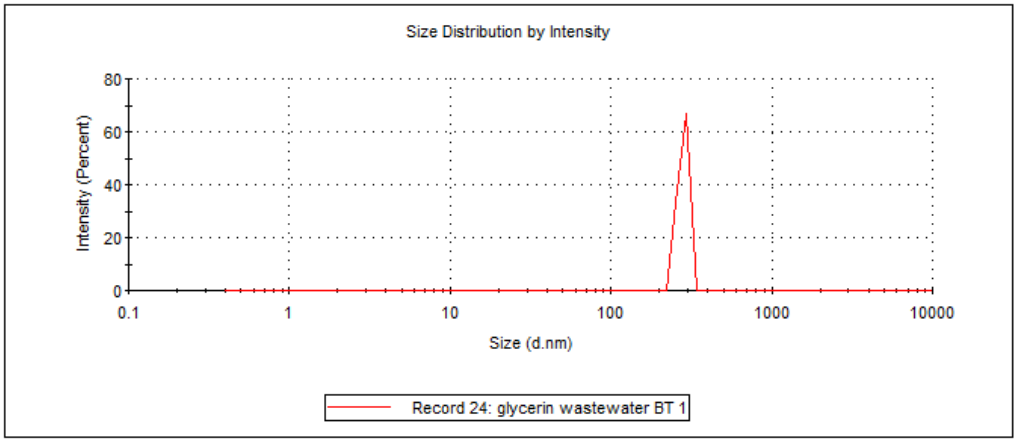

Figure 4-17 Size distribution of Glycerin WW by DLS

4.3.2.2 DLS inquiry of glycerin treated by SPIONs@ PEG

The agglomerated size of contaminant particles in glycerine WW sample were measured by DLS. The resulted curve demonstrated a reduction in density and variation in size of treatment with SPIONs@ PEG NPs. Figure 4-18 shows the average cluster size of glycerine contaminants and magnetic NPs with the size of 403 nm with the intensity percentage of 43% that demonstrates declining in the amount of the contaminant even in cluster formation around the MNPs. The amount of Z-average, as it expected, is 764 nm while PDI is 0.53. This uniformity structural cluster would be a proof of the efficiency of magnetic properties of this size NP for adsorbing the particles in unique size distributed fraction.

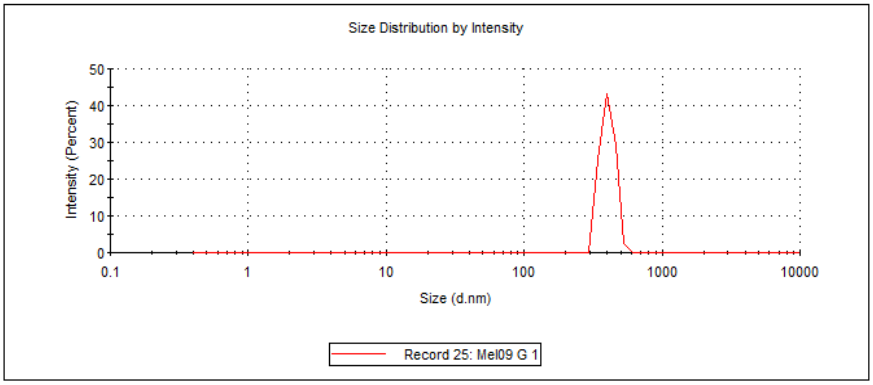

Figure 4-18 size distribution of glycerine treated with SPIONs@ PEG by DLS

4.3.2.3 DLS probe on glycerin treated by SPIONs/GO@PEG

In this case like before DLS analysis, this technique provided information of mean size distribution base on density and number distribution. DLS measurement, Figure 4-19 revealed that relatively narrow size distribution with an average size of 252 nm and 38% intensity for glycerine contaminants NPs. This size is much less than previous MNPs without GO while this volume contribution is showing increasing in the cluster size distribution in compare with the glycerine WW sample. The diameter of Z-average for this agglomeration form is 548 nm with PDI ≈ 0.5. Attendance of GO due to having active functional groups and capability to make further temporary chemical bonds lead to reduce disordering in aggregated nanoparticles.

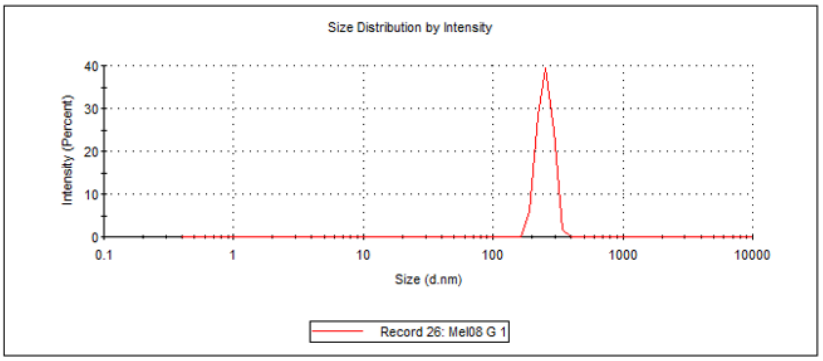

Figure 4-19 DLS analysis for glycerine treated by SPIONs/GO@ PEG

4.3.3 DLS of sugar wastewater

The resulted data from sugar WW by DLS demonstrated 289 nm for the size distribution of presence particles with Z-average of 348 nm (Figure 4-20). The coefficient correlation curve was reasonable and PDI of 0.334 for this sample in Figure 4-21. As the average particles size illustrate, all the fraction in the WW from HTC process is in nanosize. Although this amount can indicate the absolute size of the NP, agglomeration of them or even the aggregate of the particles with an appropriate affinity for this formation, the consequence dispersion form stated by the diameter size.

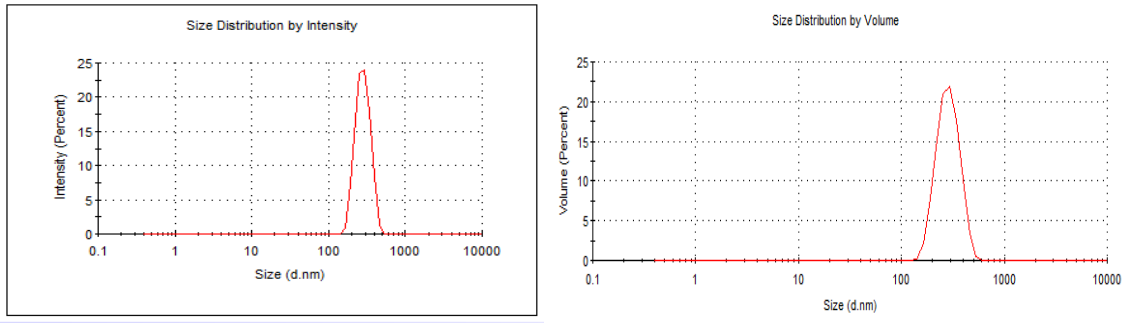

Figure 4-20 Average particles size based on density and volume of sugar WW measured by DLS

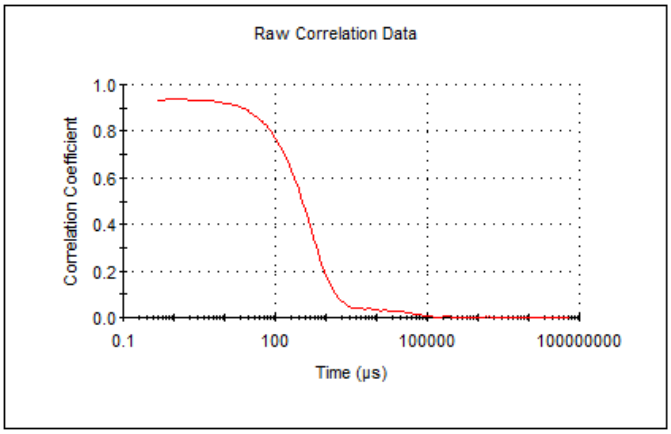

Figure 4-21 Correlation information of sugar WW by DLS

4.3.3.1 DLS study on sugar wastewater after treated by SPION@ PEG

The DLS diameter size distribution of this agglomeration particles after treatment by MNPs (SPIONs@ PEG) exposed the significant variation. The obtained results show the size of 192 nm for the agglomerated cluster which is apparently less than 289nm retained at the primary contaminant sugar particles in WW sample. Representation, the second agglomerated formation beside the main curve, may for the reason of deficiency time for removing the contaminants by magnetic treatment. The untreated sample had 24% intensity Meanwhile the treated sample by SPIONs@ PEG illustrate 17% intensity and less amount for the smaller cluster 3%. Z-average in correlated mean distribution size was 197 nm with a PDI of 0.263. The Figure 4-22 shows the DLS result of sugar sample treated by SPION@PEG.

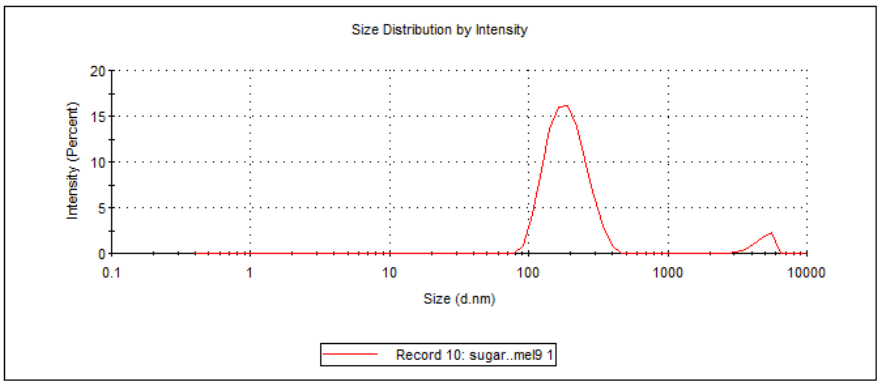

Figure 4-22 DLS curve of sugar sample after SPIONs@ PEG treatment

4.3.3.2 DLS analysis of sugar wastewater after treated by SPION/GO@ PEG

The interaction between the chemical structural of sugar with the functional group in GO induce some odd aggregation in different size and intensity. The oxygen content in a functional group of GO proposed may subsequently affect its aggregation and contaminants NP deposition on the surface of MNPs of SPIONs/GO@ PEG. Figure 4-23 shows the two clusters, one with 491 nm distribution size and the abundance of 53.8% meanwhile another peak formed in 184nm and 46.2% abundance. These results demonstrate the one big cluster which should be removed by external magnetic power, here, due to not spending sufficient time for removal, low precision or low strength of magnet this collection of NPs remained. Another assemblage reveals the interaction of between the SPIONs/GO@PEG with sugar NPs in WW whereas the functional groups over GO with oxygen bond in SPIONs constitute new interactions that lessen the diameter distribution.

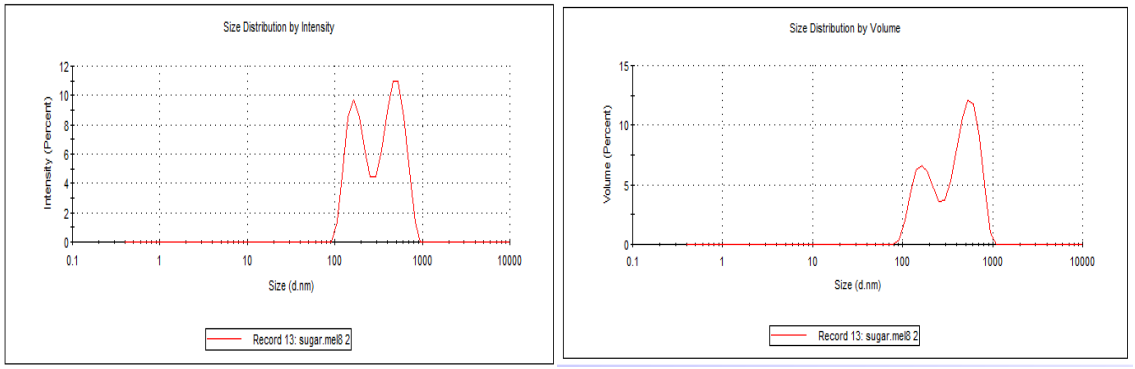

Figure 4-23 DLS measurement of sugar WW sample treated by SPIONs/GO @PEG regarding volume and density

The Z-average of the particles was reveal around 398 nm and a low PDI of 0.425. This technique may indicate a decrease in the volume percentage of cluster mass from 23 % to 6.5% and 12% for the treated particles. That means smaller particle groups represent less volume amount than another particle.

4.3.4 Atomic Force Microscopy measurement (AFM)

The physical structure of NP involved in WW consist of size, and morphology have been examined by (AFM). High-resolution AFM study of micro patterned presence NPs in WW samples prior any treatment and after the treatment to probe the significant morphology difference is desirable.

4.3.4.1 AFM analysis of glycerine wastewater sample

The glycerine sample imaged using AFM for Canada, (Bruker, Santa Barbara). All the sample were drop-deposited onto freshly cleaved mica and allowed to stay in the room temperature before imaging. They were obtained in Peak Force Taping mode. The scans were performed with the rate of I Hz speed using etched silicon cantilevers (ACTA from AppNano). The tip radius for measurement was less than 10 nm while the spring constant ≈ 42 N/m.

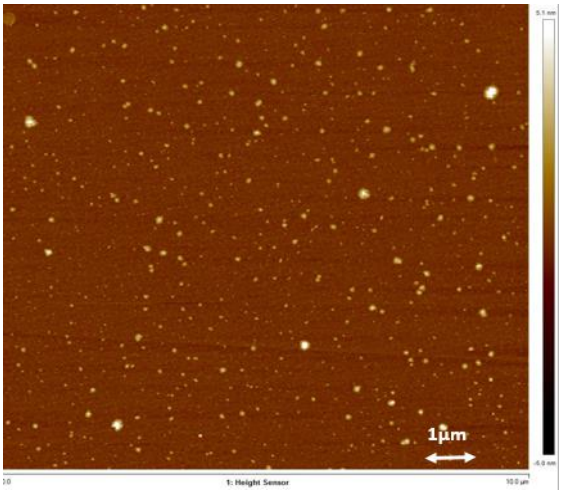
1µm

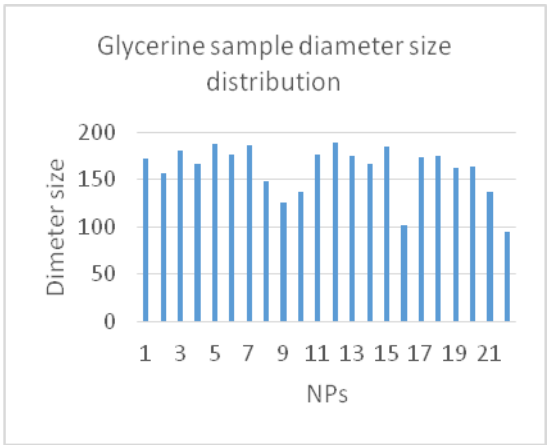
Glycerine sample diameter size distribution
Dimeter size
200
150
100
50
0
1 3 5 7 9 11 13 15 17 19 21
NPs

(a) (b)


7
6
5
4
3
2
1
%
2
4
6
8
10
12
14
nm

(c)

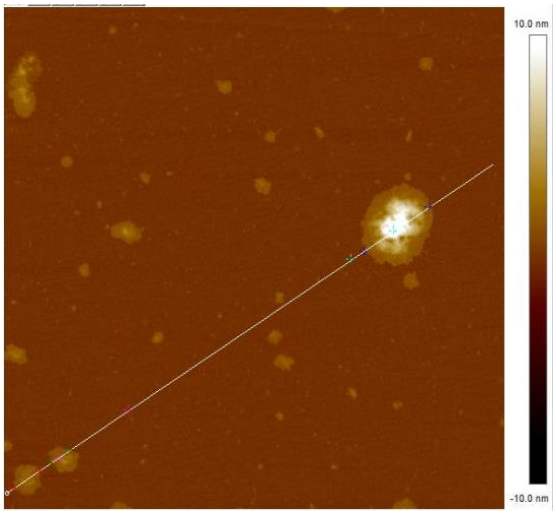
10.0 nm
-10.0 nm

(d)

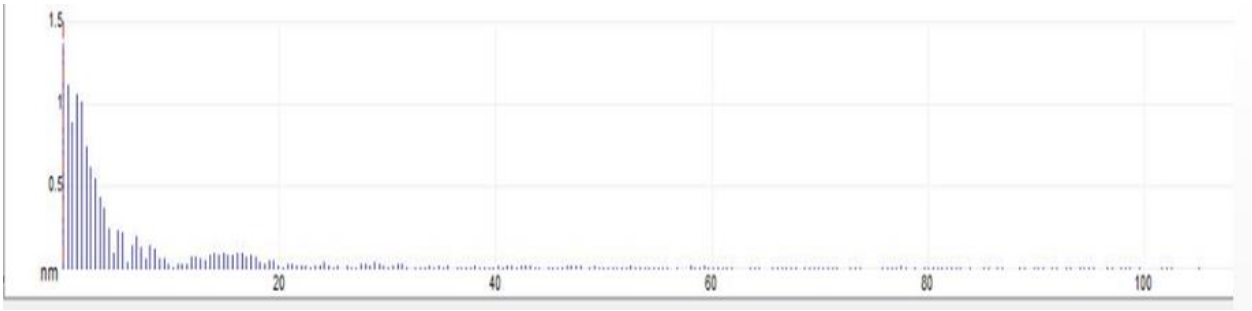

(e)

Figure 4-24 (a) AFM image of glycerine, (b) diameter size distribution histogram from glycerin sample, (c) indicating the depth histogram of glycerine particles among 520 of histogram bins, (d) AFM image of glycerine sample from different area include some huge cluster, (e) distribution histogram of represent particles in selected line in image (d).

Table.5 illustrates glycerine particles data from Figure 4-24 (a) also indicates the average diameter of represent particles in this image. The distribution of the particles clarifies the configuration deposition of the particles in separately and in aggregated form due to feasibility chemical bonding besides van der Waals interaction of NPs.

Table 5 Description the glycerin WW NPs data from AFM image of above

Parameter	Mean	Minimum	Maximum	Sigma
Total Count	83.000	83.000	83.000	0.000
Density	0.830 (/μm^2)	0.830 (/μm^2)	0.830 (/μm^2)	0.00 (/μm^2)
Height	4.033 (nm)	2,330 (nm)	14.477 (nm)	1.824 (nm)
Area	16651.4 (nm^2)	9536.75 (nm^2)	73623.65 (nm^2)	10214.55 (nm^2)
Diameter	141.292 (nm)	110.193 (nm)	306.171 (nm)	35.183 (nm)

4.3.4.2 AFM measurement of sugar

The typical image of sugar sample was taken by a Multimode Nanoscope III (Brucker, CA, USA), in Tapping Mode (or Intermitted Mode). All the image for this sample was taken using a regular probe model TESPA7 (Veeco) with a nominal spring constant of ≈ 20-80 N/m while the resonance frequency was 291-326 kHz. AFM tip touches the sample surface with beats of similar amplitude to the resonance amplitude of the AFM cantilever.

The sample imaged in the Figure 4-25 representative topography of NPs in individual mode or aggregated. The picture of the sugar WW obtained by depositing 1 µL of sugar WW in distilled water for sampling. The corresponding statistical analysis of the size, height, and another cross section profiles, as reported, follows in Table 6.

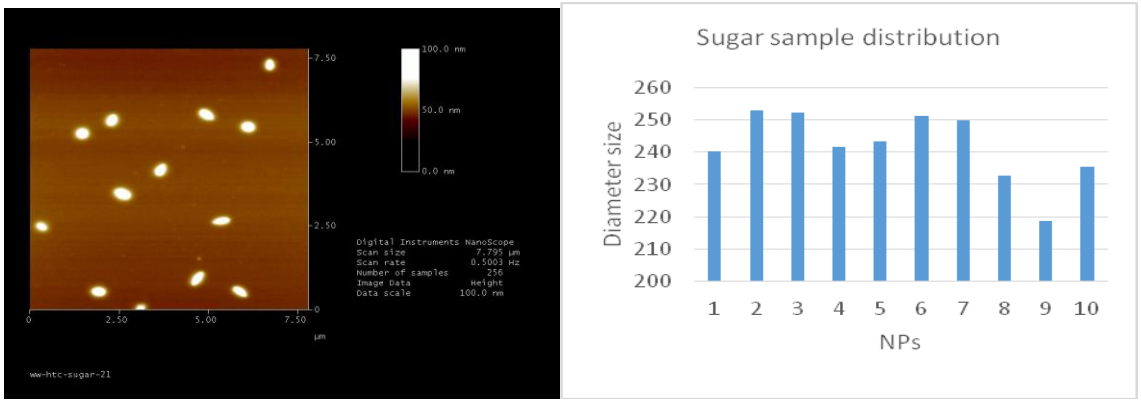

(a) (b)

Figure 4-25 (a) AFM image from topography of sugar WW prior any treatment (b) diameter size distribution of sugar sample

Table 6 Description the sugar WW NPs data from AFM

Parameter	Mean	Minimum	Maximum	Sigma
Height	62.364 (nm)	50.899 (nm)	78.606 (nm)	10.070 (nm)
Area	91347 (nm^2)	60731 (nm^2)	134211 (nm^2)	18338 (nm^2)
Diameter	339.33(nm)	278.07 (nm)	413.38 (nm)	34.147 (nm)

Length	430.69 (nm)	328.66 (nm)	517.87 (nm)	58.141 (nm)
Width	278.67 (nm)	220.69 (nm)	339.80 (nm)	40.189 (nm)

The samples were well-dispersed across the mica surface. It illustrates some extended, shapeless group NPs while losing the real natural shape of the particles is observable. As AFM images exhibit, they have a spherical, oval shape with the mean height of 62 nm and the average diameter totally 339 nm for the NP in this sample. The aggregated particle with different morphology perceives in Figure 4-26.

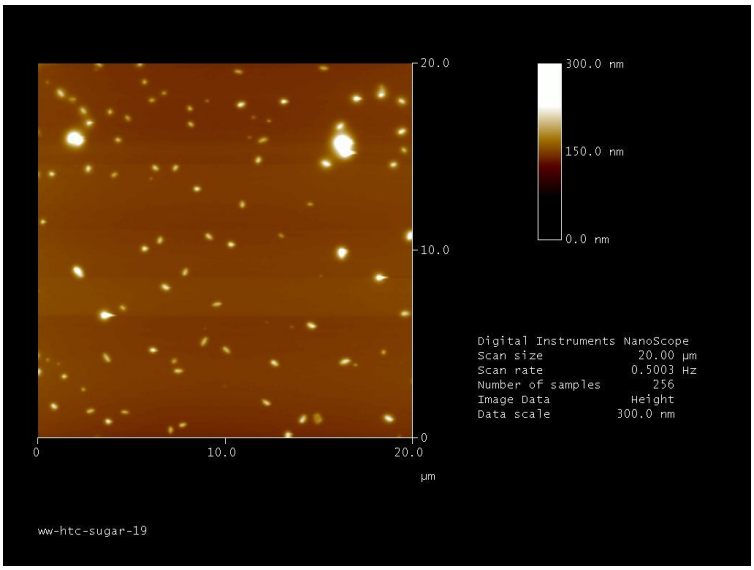

Figure 4-26 AFM image of sugar NPs indicates the presence of aggregated mass between the individual particles.

By low pass filtering, prior to the particle analysis may reduce background noise and highlight the object of interest. The images in Figure 4-27 (a, b) demonstrates the variation of particle topography with previous ones.

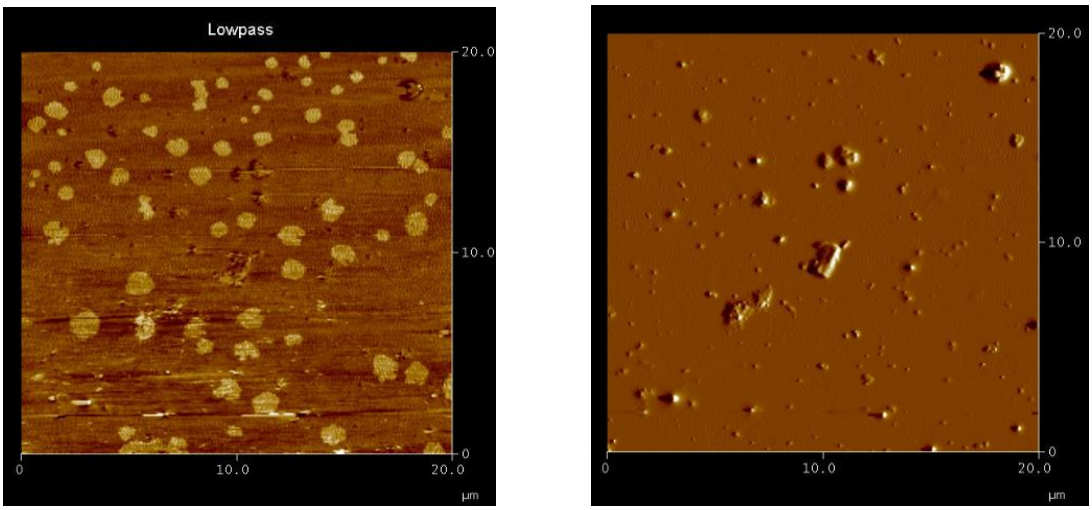

(a) (b)

Figure 4-27 (a) low pass image of sugar WW in Angel data scan of 50° (b) Height of sugar NPs with image amplitude of 1.000 v.

4.3.4.3 AFM inquiry of treated glycerine sample by SPIONs@PEG

The morphology and structure of the obtained WW sample after exposure MNPs for adsorption contaminated particles thoroughly analyzed by AFM observations. The image and correlated data were achieved using AFM for Canada, (Bruker, Santa Barbara). The scan was done at the rate of I Hz speed using etched silicon cantilevers (ACTA from AppNano). The tip radius for measurement was less than 10 nm while the spring constant ≈ 42 N/m. The analysis was carried out on dried sample by the aid of room temperature. Figure 4-28 shows the morphology of the NPs aggregation and dispersion of each cluster upon studying on the thickness of NP after contacting with MNPs.

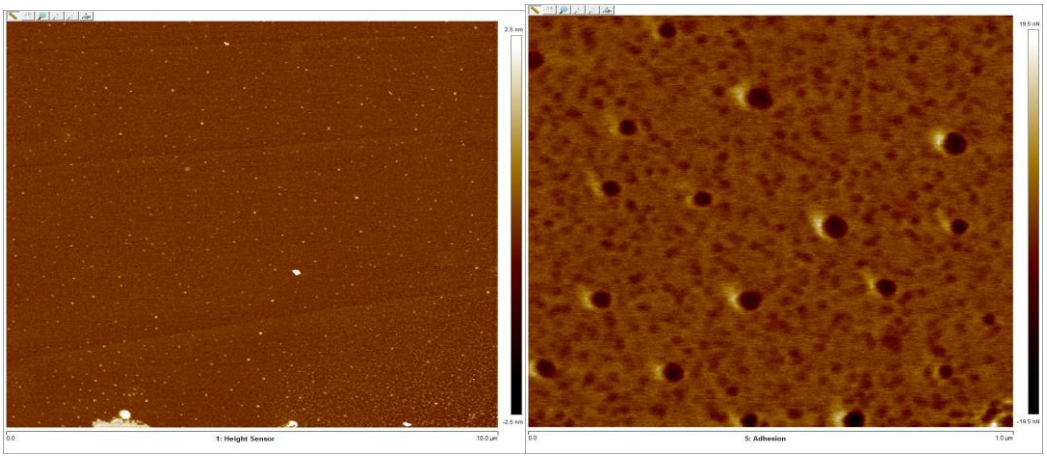

Figure 4-28 AFM images of treated glycerine WW by SPIONs@ PEG

As it shown in the Figure 4-29 (a) there are various aggregated cluster in the sample that can virtually indicate the presence of individual contaminant particles in less concentration of MNPs without any interaction with contaminant particles. Considering that the amount of NPs that chose to evaluate was 15, and among this statistical population these data were obtained. Table 7 implicates the diameter distribution of mean particles for approximately 42 nm. These result may be explained by organic interaction MNPs oxygen content and possess high adsorption affinity with contaminant NPs include hydroxyl groups. Owing to magnetite power field may remove significantly and accumulate NPs by hand laboratory magnet.

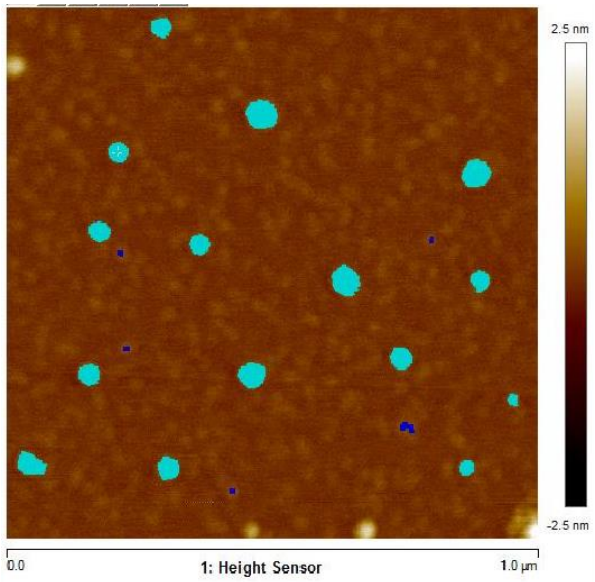

Figure 4-29 Image of particles in treated glycerine WW sample by SPIONs@ PEG

Table 7 Detail information of accumulated mode of representing NPs indicated in light blue color

Parameter	Mean	Minimum	Maximum	Sigma
Total Count	15.00	15.00	15.00	0.00
Density	15.000 (/µm^2)	15.000 (/µm^2)	15.000 (/µm^2)	0.000 (/µm^2)
Height	1.607 (nm)	0.770 (nm)	2.112 (nm)	0.338 (nm)
Area	1454.163 (nm^2)	343.323 (nm^2)	2605.438 (nm^2)	597.439 (nm^2)
Diameter	42.020 (nm)	20.908 (nm)	57.596 (nm)	9.262 (nm)

4.3.4.4 AFM analysis of glycerine sample after SPION/GO@ PEG treated

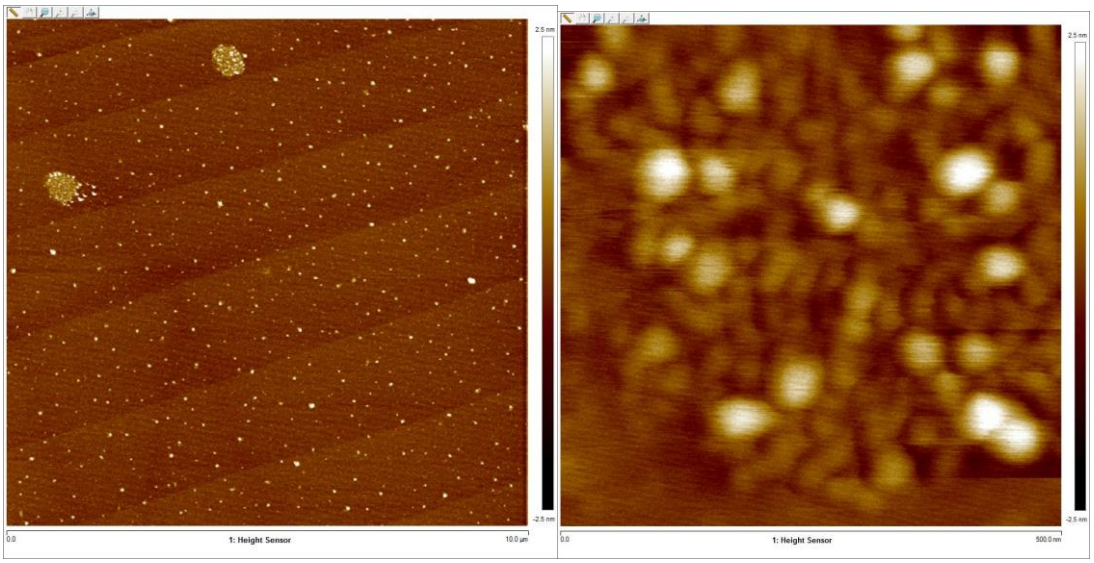

Figure 4-30 AFM images of NPs in glycerine WW in the presence of SPIONS/GO@ PEG after eliminating particles by external magnet field.

As Figure 4-30 shows, they appear to have the spherical shape as well as it seems to have a rough surface. It is clear that the form of particles change during aggregation and agglomeration, particularly when they have made a significant accumulated cluster. Figure 4-31 demonstrated morphology characteristic of the chosen NPs from the Figure 4-32 (a) among the plenty of other ones. Following the information in Table 8 the density of these selected particles (mean; 0.16 /μm^2) and size distribution of them (mean; 123nm) are revealed. This point should be noted that among the chosen bins in the image (in light blue color), some assemblage of particles observed which could simply impact the average diameter of the existent NPs.

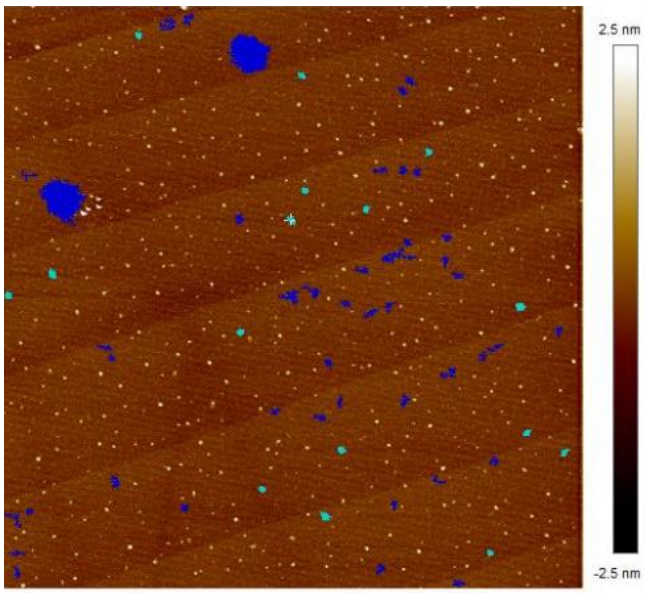

(a)

(b)

Figure 4-31 (a) AFM image of direct measure of total particle diameter and height irrespective of axis orientation of glycerine after treatment of SPIONs/GO@PEG (b) particles diameter histogram

Table 8 Particle data information by respect of defined particle to 16 for getting a result

Parameter	Mean	Minimum	Maximum	Sigma
Total Count	16.000	16.000	16.000	0.000
Density	0.160 (/μm^2)	0.160 (/μm^2)	0.160 (/μm^2)	0.000 (/μm^2)
Height	3.019 (nm)	1.786 (nm)	6.974 (nm)	1.332 (nm)
Area	12183.189 (nm^2)	9536.743 (nm^2)	19454.957 (nm^2)	2912.905 (nm^2)
Diameter	123.741 (nm)	110.193 (nm)	157.387 (nm)	14.153 (n

4.3.4.5 AFM images of sugar sample treated with SPION@ PEG

Figure 4-32(a) shows the typical AFM images of sugar WW after exposure to SPIONs@ PEG with a lateral dimension on the micrometer scale. The flat surface of sugar media is dotted with protruding particles without explicitly visible boundary. As Figure 4-32(b-c) indicates, it can estimate the average thickness and diameter of the NPs as were done by determined light blue spots.

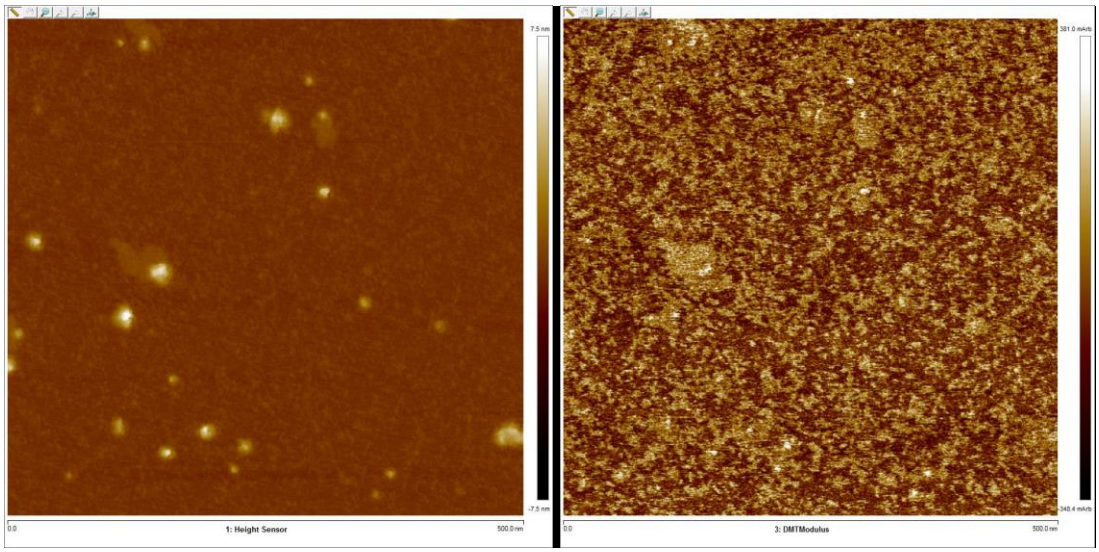

(a)

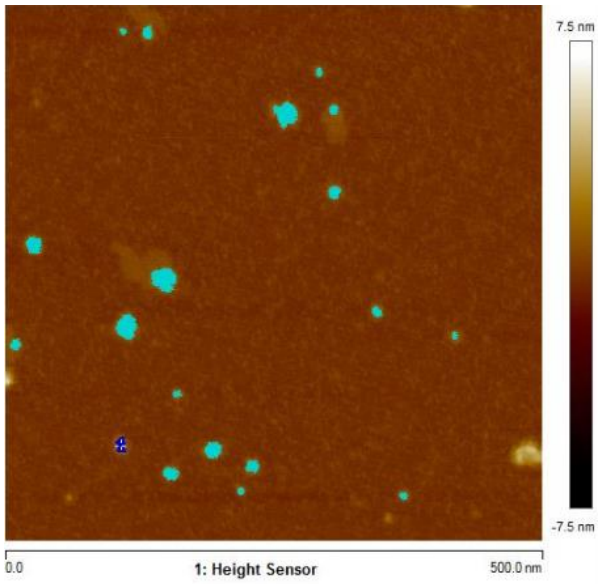

(b)

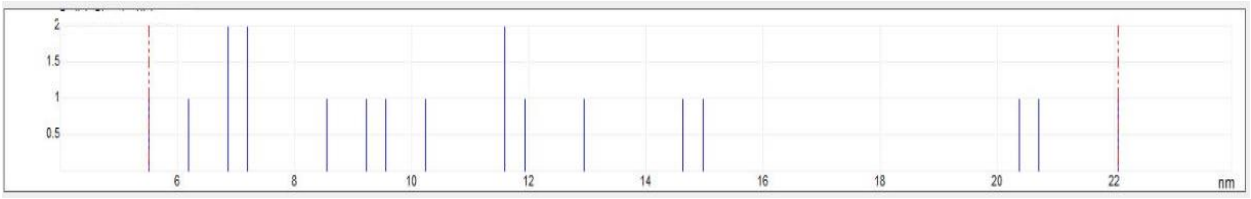

(c)

Figure 4-32 Typical AFM image of sugar treated by SPIONs@ PEG (b) AFM image of lateral dimension of NPs in sugar WW after adsorption contact to SPIONs@ PEG (c) particle diameter histogram

Table 9 data assessment from light spot in image of sugar sample treated with SPION@ PEG

Parameter	Mean	Minimum	Maximum	Sigma
Total count	27.000	27.000	27.000	0.000
Density	108.000 (/μm^2)	108.000 (/μm^2)	108.000 (/μm^2)	0.000(/μm^2)
Height	2.291 (nm)	1.227 (nm)	5.800 (nm)	1.067 (nm)
Area	71.526 (nm^2)	24.796 (nm^2)	316.620 (nm^2)	63.924(nm^2)
Diameter	8.903 (nm)	5.619 (nm)	20.078 (nm)	3.436 (nm)

4.3.4.6 AFM analyze of treated sugar wastewater by SPIONs/GO@ PEG

Figure 4-33 shows AFM images the sugar WW sample after exposure to MNPs of SPIONs/GO@ PEG. The size of each NP represented in the medium was evaluated to be approximately 8.9 nm in diameter limited by some selected light blue color spot in the related image in Figure 4-35(a).

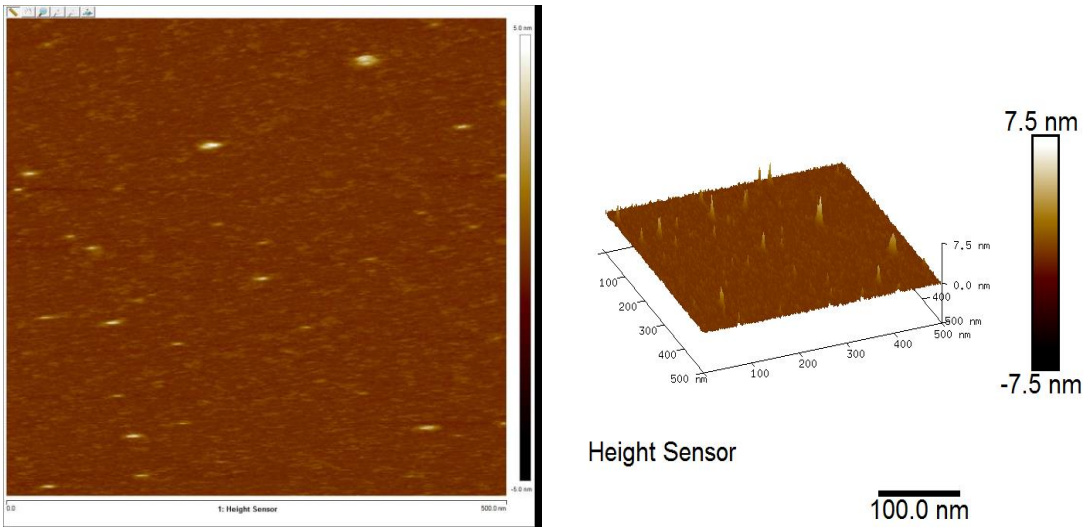

Figure 4-33Tapping mode of AFM image of sugar sample treated by SPIONs/GO @ PEG

The average diameter estimated for sugar contaminants NPs could not adopt with our previous information data for sugar sample NP ahead of treating by MNPs. The real size of sugar NP is virtually less than 10 nm. As we expected the sugar particles setteled down on the sheet of GO due to atendance of these particle in samples after treatment and magnetic removal. Therefor elliptical shape for each particle or collected particles can observe. Based on AFM evidence, first, the diameter of the individual or few aggregated SPIONs/GO @ PEG, MNPs, with sugar WW sample evaluated as an average 8.9 nm in the XY-plane and ≈3.02 nm of height by the z-plane thickness. The density of the remained particle in sample changed to 72 (μm^{-2}) which shows less congestion of contaminant in compare with treatment with SPIONs@ PEG (density of sample after treatment 108 (μm^{-2}). It demonstrate the higher efficiency of the

SPIONs/GO@PEG in compare with SPIONs @PEG for adsorption nanocontaminat and removal.

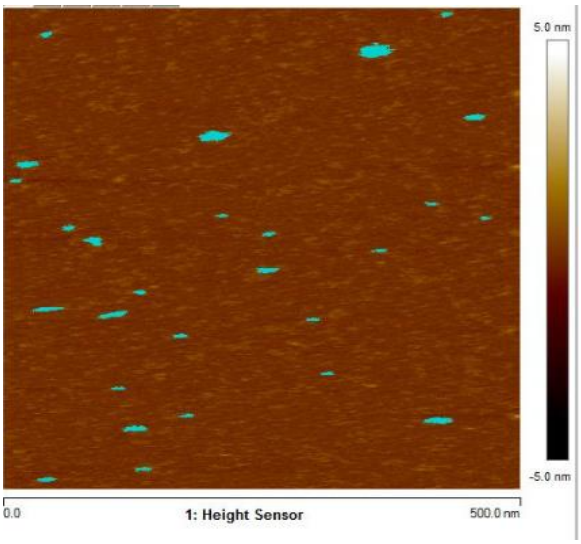

(a)

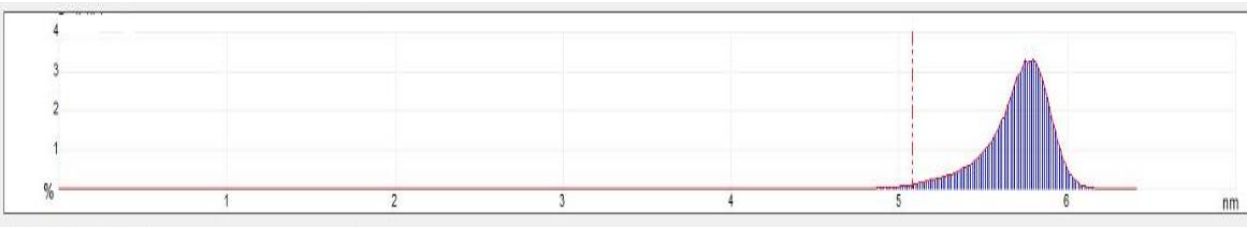

(b)

Figure 4-34 (a) Tapping mode AFM images of sugar sample after treated by SPIONs @ PEG with selected light blue for evaluation the data (b) illustration depth of particles histogram

Table 7 obtained result from 27 NPs of sugar sample after treatment by SPIONs/GO @ PEG

Parameter	Mean	Minimum	Maximum	Sigma
Total count	18.000	18.000	18.000	0.000
Density	72.000 (/μm^2)	72.000 (/μm^2)	72.000 (/μm^2)	0.000(/μm^2)
Height	4.347 (nm)	2.362 (nm)	7.192 (nm)	1.341 (nm)
Area	123.607 (nm^2)	23.842 (nm^2)	382.423 (nm^2)	110.476(nm^2)
Diameter	11.466 (nm)	5.510 (nm)	22.066 (nm)	5.090 (nm)

CHAPTER 5: GENERAL DISCUSSION

The objective of this project is to apply the widespread efficiency of nanotechnology to remove contamination in nanoscale from the liquid fraction of HTC through iron oxide NPs. These magnetite NPs provide a favorable condition to execute adsorption and take away unwilling particles from the milieu by means of magnetic force field. Here, we preferred to utilize SPIONs as an unprecedented excellent material due to its most fundamental properties. The presence of iron oxides in the core of particle made it as a targeted supplementary beside the nano scale dimension of the NPs. The supermagnetism of the particles extend their application through manipulation and control after using an external magnetic field. Considering to this point, that the WW and sludge engineerings are reversible sources of energy, pouring money and studies into this field could be beneficial because of the potential energy and material it carries.

By this approach, inquiry on the liquid phase of HTC process, as an applicable and plentiful water source which generate by HTC (as one of the controversial techniques) seems profitable. So far just a few researchers have probed on this field efficiently. In this study, we synthesized SPIONs with a layer of high weighted PEG (20000 Da) for further prevention oxidation which may lead to losing the crystalline structure of the magnetite particles as first MNPs. Second, providing NPs pertinent to the loading of GO on SPION for preparing multifunctional MNPs. Both of these hybrids may exhibit unique properties for adsorption contaminants. They can congregate under the acidic condition that we have originally for the products after HTC. Aggregated hybrid by the aide of PEG (20000 Da) can be dispersed well in sonication condition. These properties can compel these NPs to remove contaminant NPs in our waste samples and remove them by a medium external power of enough powerful magnet. This approach was executed on two samples from glycerine and sugar produced via HTC process. However, one of the limitations for proceeding from this strategies is the nanocomposite affinity to aggregation and agglomeration. The high potential of this NP for adsorbing particles and suspended contaminant fractions in the WW sample can advance our goal. The FT-IR peaks confirmed the presence of initial material like glycerine, and sugar samples, precisely. Therefore, the main subject for contaminant elimination was nanostructural hydrocarbon substances. The UV-vis spectroscopy demonstrated reasonable reduction of contamination after exposure to SPIONs@

PEG. Since the hybrid of SPIONs/GO@ PEG NPs due to large number of functional groups oxygen content, didn't exhibit significant difference from relevant untreated sample. The main expected peaks for adsorption functional groups are around (200-300cm^{-1}) that may adopt with UV-vis spectra of primary samples and other active functional groups in GO. For inquiring on the size distribution of synthesized NPs, DLS techniques also revealed their variation of stabilizations in the aggregation position. The average diameter size of cluster is respectively 548 nm for SPION@PEG and 242 nm for SPIONs/GO@PEG. These data are corresponding with the virtual position and configuration of the oxygen bonding between the functional groups of GO sheets and magnetite iron oxides, which make them well arranged crystalline form in comparison to the SPIONs@PEG. Diluted synthesized samples in AFM images confirm this claim for arranging the particles in the presence of GO. Low aggregated particles in SPIONs @PEG and SPIONs/GO@PEG in AFM images indicate 40.5nm and 36.9nm in respect for each NCs. GO represented some prevention for further agglomerating for SPIONs due to the active site on the graphene sheet and make more ordering in configuration of the clusters. As our expectation for TEM images, these differences could be observed. SPIONs @PEG reveal almost 11.4 nm for real diameter while as it was less for nanohybrid of SPIONs/GO@PEG. This point should be mentioned that the calculation of average distribution diameter of NPs is strongly dependent of the selection point and area of taking the image. This issue is significant in AFM images of the WW samples as well as the synthesized NCs and WW after hybrid magnetite treatment. For clarifying the results of glycerin WW before and after treatment may state same consequences, the diameter distribution for glycerine WW was 281.8 nm which changed the diameter and intensity of cluster after the treatment. Relevant results were obtained by both DLS and AFM techniques. The size of remained aggregated glycerine WW particles were 403 and 252 nm with 43% and 38% reduction in the amount of contamination for SPIONs@ PEG and SPIONs/GO@PEG respectively The diameter of each measured cluster after treatment by exposure to SPIONs can be affected by the magnetite chemical structure and by nanocontaminants. In the case of sugar sample; almost 33 % and 60% reduction in the percentage of the intensity observed after treatment with SPIONs@PEG and SPIONs/GO@PEG respectedly which lead to decreasing of absolute nano contaminant particles. This reduction could define by the new structural configuration of oxygen bonding and effective interaction between the functional groups in sugar with SPIONs /GO@ PEG. Definitely, other remained

NPs might be removed by repeating the treatment for many times. Obviously, insufficient required time for trapping the adsorbed groups by hand laboratory magnet may impact or effect the treatment WW involved nanocontaminats with SPIONs.

Ingeneral, two parameters can potentially induce the reduction of nano contaminants in WW samples, the nano size of iron oxide effects and the presence of oxygenated bonds in contaminant particle that promote adsorption attraction for temporary bonds for leading the elimination from the liquid. Moreover, the feasibility to manipulate the particles after loaded with contaminants by an external magnet is a dominent aspect in this research.

AFM images of the treated samples by two kinds SPIONs confirmed the result of DLS. At this analysis stage, no effort was done to get the outcome with a particular orientation. Therefore, the evaluation was performed not only with comparing the data before and after the treatment but also stand on the other evidence from the analyses. For example in glycerin WW analysis after treatment by SPIONs@ PEG, AFM images in respect to randomize selected area including the particles, assess 42.02 nm for diameter distribution. Whereas, this same evaluation demonstrate 123 nm after treatment with SPIONs /GO@PEG. Considering this point that the operator choose the largest aggregated particles among the others for appraising though last images. Therefore, the average accuracy size of the remained NPs was effected by this selection. In sugar WW, the qualification of determined AFM images certified the reduction and alteration in diameter size in whole. The initial sugar WW exhibited 339nm mean diameter of the particle for contaminates meanwhile this amount reduced to 8.9 nm and 11.4 nm after treated by SPION@PEG and SPIONs/GO@ PEG respectively. The shape of particles in the first case is spherical due to the recombination with spherical SPIONs@ PEG and for the second item, all the particles appear as elliptical NPs that represent attendance of GO sheet in these nanoparticles structure. The reduction contaminants can observe in preliminary experiments before further analysis so that even the naked eyes can distinguish the color alteration and modification in transparency of the liquid after treatment of samples by SPIONs.

CHAPTER 6: CONCLUSION AND RECOMMENDATION FOR FUTURE RESEARCH

The main novelty of this study stands on the capability of SPIONs derives to trap and remove contaminants by potentially magnetite properties during treatment of WW. Considering the economic simplicity and cost-effective points of nano structured materials application besides the high potential for reversibility performance make them favorite candidate. In recent years, HTC represents an environmental, eco-friendly, energetically efficient process for various biomass and natural WW which is used in many developed countries such as Germany. The liquid part sequestered requires more research potentially to recover the nutrients or other valuable hydrocarbons (Libra et al. 2011). The high pressure and temperature destroy pathogens and other pharmaceutical compounds in this phase as well as others insisted before (Sütterlin, Trittler et al. 2007). But it has a potential to transfer heavy metals or some other small hydrocarbons from the initial feedstock.

In this work, we synthesized two derived of SPIONs with high molecular weight of PEG to display their application for contaminant removal from WW via HTC method. By this way we may reach the valuable source of water which usually discard without remarkable studies on it.

The originality of this work can thus be summarized as follows:

- ✓ Synthesis of SPIONs@ PEG and SPIONs/GO@ PEG as the two magnetite NPs by iron compounds under nitrogen gas atmosphere.
- ✓ Analysis of the synthesized magnetite particles for structural approval.
- ✓ Examination of the WW samples for functional groups determination.
- ✓ Exposure of SPIONs to the principal samples for treatment based on adsorption.
- ✓ Various Spectroscopy and microscopy tests for further analyzing the samples in initial and treated cases.

Several recommendation for treatment of WW from HTC are drawn from this master's project.

- The forthcoming steps are biocompatibility tests of fabricated NPs on plants and simple animals such as Limna and Hydra to evaluate the viability lifetime of them after exposure with MNPs. These tests provide a perspective sight for consuming of the nanotechnology for remediation the WW in large scale. Additional information may obtain by investigation on the qualification of the ecosystem and different organism about their persistence is vital for further study.
- Next recommendation pertains to the functionality of these fabricated NPs for the treatment of WW consist of widespread environmental bacteria such as E. coli, K12. If these particles would be capable to impact on the viability of these bacteria, it may possible to employ them individually or as the modified supplement match to the other part of the WW treatment plant.
- We recommended strongly for portability test of HTC WW samples. As far as mentioned before, there are not significant dangerous materials in this part of WW but heavy metals can represent exceptionally. WW produced via HTC still needs to research about nontoxicity and safety for animal drinking.

- This project can implement for an infrastructure treatment plant of WW and affluent from HTC after a complete investigation for scale up from the laboratory proposal as beneficial remediation design. Contriving an appropriate coil magnet as an external magnet force for catching the associated contaminants with SPIONs through the way of effluent flow may remove particles better from WW.

- All metals may create concerning the human life and ecosystem adverse impact so monitoring the presence heavy metals in this part are suggested. These heavy metals may include arsenic, chromium, lead, and mercury.

- Repeating the experimental stages for treatment may induce further appropriate consequence by employing these SPIONs as nano contaminant removal.

REFERENCES

A Funke, F. Z. (2010). "Hydrothermal carbonization of biomass: a summary and discussion of chemical mechanisms for process engineering." Biofuels, Bioproducts and Biorefining. **4**: 160-177.

Ahmed, F. and D. F. Rodrigues (2013). "Investigation of acute effects of graphene oxide on wastewater microbial community: a case study." Journal of hazardous materials **256**: 33-39.

Ahmed, S., et al. (2011). "Influence of parameters on the heterogeneous photocatalytic degradation of pesticides and phenolic contaminants in wastewater: a short review." Journal of environmental management **92**(3): 311-330.

Ai, L., et al. (2011). "Removal of methylene blue from aqueous solution by a solvothermal-synthesized graphene/magnetite composite." Journal of hazardous materials **192**(3): 1515-1524.

Ambashta, R. D. and M. Sillanpää (2010). "Water purification using magnetic assistance: a review." Journal of hazardous materials **180**(1): 38-49.

Andersson, D. I. (2003). "Persistence of antibiotic resistant bacteria." Current opinion in microbiology **6**(5): 452-456.

Arques, A., et al. (2007). "Detoxification and/or increase of the biodegradability of aqueous solutions of dimethoate by means of solar photocatalysis." Journal of hazardous materials **146**(3): 447-452.

Bakshi, D. K. and P. Sharma (2003). "Genotoxicity of textile dyes evaluated with Ames test and rec-assay." Journal of environmental pathology, toxicology and oncology **22**(2).

Baquero, F., et al. (2008). "Antibiotics and antibiotic resistance in water environments." Current opinion in biotechnology **19**(3): 260-265.

Belgiorno, V., et al. (2007). "Review on endocrine disrupting-emerging compounds in urban wastewater: occurrence and removal by photocatalysis and ultrasonic irradiation for wastewater reuse." Desalination **215**(1): 166-176.

Berge, N. D., et al. (2011). "Hydrothermal carbonization of municipal waste streams." Environmental science & technology **45**(13): 5696-5703.

Brandes, M. (1978). "Characteristics of effluents from gray and black water septic tanks." Journal (Water Pollution Control Federation): 2547-2559.

Bystrzejewski, M., et al. (2009). "Carbon-encapsulated magnetic nanoparticles as separable and mobile sorbents of heavy metal ions from aqueous solutions." Carbon **47**(4): 1201-1204.

Can, O., et al. (2006). "Treatment of the textile wastewater by combined electrocoagulation." Chemosphere **62**(2): 181-187.

Chan, K. T., et al. (2008). "First-principles study of metal adatom adsorption on graphene." Physical Review B **77**(23): 235430.

Chandra, V., et al. (2010). "Water-dispersible magnetite-reduced graphene oxide composites for arsenic removal." ACS nano **4**(7): 3979-3986.

Chen, Y., et al. (2005). "Preparation of a novel TiO2-based pn junction nanotube photocatalyst." Environmental science & technology **39**(5): 1201-1208.

Crook, J., et al. (1999). "Potable use of reclaimed water." Journal of the American Water Works Association **91**(8).

Dasari, M. A., et al. (2005)."Low-pressure hydrogenolysis of glycerol to propylene glycol." Applied Catalysis A: General **281**(1): 225-231.

Deng, J.-H., et al. (2013). "Simultaneous removal of Cd (II) and ionic dyes from aqueous solution using magnetic graphene oxide nanocomposite as an adsorbent." Chemical Engineering Journal **226**: 189-200.

Dixon, A. M., et al. (1999). "Guidelines for Greywater Re-Use: Health Issues." Water and Environment Journal **13**(5): 322-326.

Drewes, J. E., et al. (2005). "An assessment of endocrine disrupting activity changes during wastewater treatment through the use of bioassays and chemical measurements." Water Environment Research: 12-23.

Dwight, D. J., et al. (1985). "Manual of Mineralogy." Wiley, New York: 276.

Environmental Canada (2015). "waterpollution, wastewater (HAI)."

Environmental National Geographic (2015). "Freshwater crisis(HAI)."

Eriksson, E., et al. (2002). "Characteristics of grey wastewater." Urban water **4**(1): 85-104.

Eriksson, E., et al. (2007). "Risk assessment of xenobiotics in stormwater discharged to Harrestrup Å, Denmark." Desalination **215**(1): 187-197.

Escala, M., et al. (2012). "Hydrothermal carbonization as an energy-efficient alternative to established drying technologies for sewage sludge: a feasibility study on a laboratory scale." Energy & Fuels **27**(1): 454-460.

Fan, X., et al. (2008). "Deoxygenation of exfoliated graphite oxide under alkaline conditions: a green route to graphene preparation." Advanced Materials **20**(23): 4490-4493.

Funke, A. and F. Ziegler (2010). "Hydrothermal carbonization of biomass: a summary and discussion of chemical mechanisms for process engineering." Biofuels, Bioproducts and Biorefining **4**(2): 160-177.

Fytili, D. and A. Zabaniotou (2008). "Utilization of sewage sludge in EU application of old and new methods—a review." Renewable and Sustainable Energy Reviews **12**(1): 116-140.

Gao, Y., et al. (2012). "Adsorption and removal of tetracycline antibiotics from aqueous solution by graphene oxide." Journal of Colloid and interface Science **368**(1): 540-546.

Garabrant, D. H., et al. (1992). "DDT and related compounds and risk of pancreatic cancer." Journal of the National Cancer Institute **84**(10): 764-771.

Gautier, J., et al. (2012). "A pharmaceutical study of doxorubicin-loaded PEGylated nanoparticles for magnetic drug targeting." International journal of pharmaceutics **423**(1): 16-25.

Gilchrist, R., et al. (1957). "Selective inductive heating of lymph nodes." Annals of surgery **146**(4): 596.

Gillesby, B. E. and T. R. Zacharewski (1998). "Exoestrogens: mechanisms of action and strategies for identification and assessment." Environmental Toxicology and Chemistry **17**(1): 3-14.

Gu, L., et al. (2013). "One-step preparation of graphene-supported anatase TiO2 with exposed {001} facets and mechanism of enhanced photocatalytic properties." ACS applied materials & interfaces **5**(8): 3085-3093.

Gupta, A. K. and M. Gupta (2005). "Synthesis and surface engineering of iron oxide nanoparticles for biomedical applications." Biomaterials **26**(18): 3995-4021.

Hagström, P. (2005). "Evaluation of the Biomass potential for Heat, Electricity and Vehicle Fuel in Sweden."

Hamley, I. (2003). "Nanotechnology with soft materials." Angewandte Chemie International Edition **42**(15): 1692-1712.

He, H., et al. (1998). "A new structural model for graphite oxide." Chemical Physics Letters **287**(1–2): 53-56.

Herve, K., et al. (2008). "The development of stable aqueous suspensions of PEGylated SPIONs for biomedical applications." Nanotechnology **19**(46): 465608.

Hooda, P. and B. Alloway (1994). "The plant availability and DTPA extractability of trace metals in sludge-amended soils." Science of the Total Environment **149**(1): 39-51.

Hu, H., et al. (2007). "The epidemiology of lead toxicity in adults: measuring dose and consideration of other methodologic issues." Environmental health perspectives **115**(3): 455.

Hu, H., et al. (2010). "Synthesis of monodisperse Fe 3 O 4@ silica core–shell microspheres and their application for removal of heavy metal ions from water." Journal of Alloys and Compounds **492**(1): 656-661.

Huerta-Fontela, M., et al. (2008). "Stimulatory drugs of abuse in surface waters and their removal in a conventional drinking water treatment plant." Environmental science & technology **42**(18): 6809-6816.

Ji, L., et al. (2009). "Mechanisms for strong adsorption of tetracycline to carbon nanotubes: A comparative study using activated carbon and graphite as adsorbents." Environmental science & technology **43**(7): 2322-2327.

Jiries, A. G., et al. (2002). "Pesticide and heavy metals residue in wastewater, soil and plants in wastewater disposal site near Al-Lajoun Valley, Karak/Jordan." Water, air, and soil pollution **133**(1-4): 97-107.

Junyapoon, S. (2005). "Use of zero-valent iron for wastewater treatment." Journal of KMITL Sci Tech **5**(3): 587-595.

Kim, S. D., et al. (2007). "Occurrence and removal of pharmaceuticals and endocrine disruptors in South Korean surface, drinking, and waste waters." Water research **41**(5): 1013-1021.

Knubovets, T., et al. (1999). "Structure, thermostability, and conformational flexibility of hen egg-white lysozyme dissolved in glycerol." Proceedings of the National Academy of Sciences **96**(4): 1262-1267.

Kolpin, D. W., et al. (2002). "Pharmaceuticals, hormones, and other organic wastewater contaminants in US streams, 1999-2000: A national reconnaissance." Environmental science & technology **36**(6): 1202-1211.

Kotchen, M., et al. (2009). "Pharmaceuticals in wastewater: Behavior, preferences, and willingness to pay for a disposal program." Journal of environmental management **90**(3): 1476-1482.

Kowalska, I., et al. (2005). "Removal of detergents from industrial wastewater in ultrafiltration process." Environment Protection Engineering **31**(3/4): 207.

Krishnamoorthy, K., et al. (2013). "The chemical and structural analysis of graphene oxide with different degrees of oxidation." Carbon **53**: 38-49.

Langergraber, G. and E. Muellegger (2005). "Ecological Sanitation—a way to solve global sanitation problems?" Environment international **31**(3): 433-444.

Laurent, S., et al. (2008). "Magnetic iron oxide nanoparticles: synthesis, stabilization, vectorization, physicochemical characterizations, and biological applications." Chemical reviews **108**(6): 2064-2110.

Lazar, T. (2005). Color chemistry: synthesis, properties, and applications of organic dyes and pigments, Wiley Online Library.

Lee, J., et al. (2013). "Graphene oxide nanoplatelets composite membrane with hydrophilic and antifouling properties for wastewater treatment." Journal of Membrane Science **448**: 223-230.

Li, B., et al. (2011). "Superparamagnetic Fe 3 O 4 nanocrystals@ graphene composites for energy storage devices." Journal of Materials Chemistry **21**(13): 5069-5075.

Li, X., et al. (2006). "Zero-valent iron nanoparticles for abatement of environmental pollutants: materials and engineering aspects." Critical reviews in solid state and materials sciences31(4): 111-122.

Libra, J. A., et al. (2011). "Hydrothermal carbonization of biomass residuals: a comparative review of the chemistry, processes and applications of wet and dry pyrolysis." Biofuels **2**(1): 71-106.

Liu, J.-f., et al. (2008). "Coating Fe3O4 magnetic nanoparticles with humic acid for high efficient removal of heavy metals in water." Environmental science & technology **42**(18): 6949-6954.

M Escala, T. Z., C Koller, R Junge (2012). "Hydrothermal carbonization as an energy-efficient alternative to established drying technologies for sewage sludge: a feasibility study on a laboratory scale." Energy & Fuels **27**(1) : 454-460.

Ma, L. and W.-x. Zhang (2008). "Enhanced biological treatment of industrial wastewater with bimetallic zero-valent iron." Environmental science & technology **42**(15): 5384-5389.

Mahdavian, A. R. and M. A.-S. Mirrahimi (2010). "Efficient separation of heavy metal cations by anchoring polyacrylic acid on superparamagnetic magnetite nanoparticles through surface modification." Chemical Engineering Journal **159**(1): 264-271.

Mauter, M. S. and M. Elimelech (2008). "Environmental applications of carbon-based NMs." Environmental science & technology **42**(16): 5843-5859.

Mishra, S. P., et al. (1996). "Radiotracer technique in adsorption study: Part XIV. Efficient removal of mercury from aqueous solutions by hydrous zirconium oxide." Applied Radiation and Isotopes **47**(1): 15-21.

Mittal, A., et al. (2009). "Adsorption studies on the removal of coloring agent phenol red from wastewater using waste materials as adsorbents." Journal of Colloid and interface Science **337**(2): 345-354.

Moawad, H., et al. (2003). "Evaluation of biotoxicity of textile dyes using two bioassays." Journal of basic microbiology **43**(3): 218-229.

Molina, Miguel M., et al. "Nitric oxide donor superparamagnetic iron oxide nanoparticles." *Materials Science and Engineering: C* 33.2 (2013): 746-751.

Nitschke, L. and W. Schüssler (1998). "Surface water pollution by herbicides from effluents of waste water treatment plants." Chemosphere **36**(1): 35-41.

Nitschke∗, L. and W. Schüssler (1998). "Surface water pollution by herbicides from effluents of waste water treatment plants." Chemosphere **36**(1): 35-41.

Novoselov, K., et al. (2005). "Two-dimensional gas of massless Dirac fermions in graphene." nature **438**(7065): 197-200.

Pan, B., et al. (2009). "Development of polymeric and polymer-based hybrid adsorbents for pollutants removal from waters." Chemical Engineering Journal **151**(1): 19-29.

Pandey, A., et al. (2007). "Bacterial decolorization and degradation of azo dyes." International Biodeterioration & Biodegradation **59**(2): 73-84.

Paterson, E. (1992). "Iron Oxides in the Laboratory. Preparation and Characterization." 339-393.

Petrović, M., et al. (2003). "Analysis and removal of emerging contaminants in wastewater and drinking water." TrAC Trends in Analytical Chemistry **22**(10): 685-696.

Pirkarami, A., et al. (2013). "Decolorization of azo dyes by photo electro adsorption process using polyaniline coated electrode." Progress in Organic Coatings **76**(4): 682-688.

Pousa, G., et al.(2007). "History and policy of biodiesel in Brazil." Energy Policy **35**(11): 5393-5398.

Prasad, M. N. V. (2013). Heavy metal stress in plants: from biomolecules to ecosystems, Springer Science & Business Media.

Salehi, A., et al. (2013). "Evaluating the role of industrial sludge as a source of heavy metal pollution." KAUMS Journal (FEYZ) **16**(7): 719-720.

Schaer, M., et al. (2014). "Multi-Functional Magnetic Photoluminescent Photocatalytic Polystyrene-Based Micro-and Nano-Fibers Obtained by Electrospinning." Fibers **2**(1): 75-91.

Sevilla, M. and A. B. Fuertes (2009). "Chemical and structural properties of carbonaceous products obtained by hydrothermal carbonization of saccharides." Chemistry-A European Journal **15**(16): 4195-4203.

Sevilla, M. and A. B. Fuertes (2009). "The production of carbon materials by hydrothermal carbonization of cellulose." Carbon **47**(9): 2281-2289.

Siebe, C. and E. Cifuentes (1995). "Environmental impact of wastewater irrigation in central Mexico: an overview." International Journal of Environmental Health Research **5**(2): 161-173.

Sipos, P., et al. (2003). "Formation of spherical iron (III) oxyhydroxide nanoparticles sterically stabilized by chitosan in aqueous solutions." Journal of inorganic biochemistry **95**(1): 55-63.

Snyder, S. A., et al. (2003). "Pharmaceuticals, personal care products, and endocrine disruptors in water: implications for the water industry." Environmental Engineering Science **20**(5): 449-469.

Sponza, D. T. (2002). "Necessity of toxicity assessment in Turkish industrial discharges (examples from metal and textile industry effluents)." Environmental monitoring and assessment **73**(1): 41-66.

Stankovich, S., et al. (2007). "Synthesis of graphene-based nanosheets via chemical reduction of exfoliated graphite oxide." Carbon **45**(7): 1558-1565.

Sterritt, R. and J. Lester (1980). "The value of sewage sludge to agriculture and effects of the agricultural use of sludges contaminated with toxic elements: a review." Science of the Total Environment **16**(1): 55-90.

Sullivan, R. H., et al. (1973). "Survey of facilities using land application of wastewater."

Sütterlin, H., et al. (2007). "Fate of Benzalkonium Chloride in a Sewage Sludge Low Temperature Conversion Process Investigated by LC-LC/ESI-MS/MS." CLEAN–Soil, Air, Water **35**(1): 81-87.

Tchobanoglous, G. and F. L. Burton (1991). "Wastewater engineering." Management **7**: 1-4.

Ternes, T. A. (1998). "Occurrence of drugs in German sewage treatment plants and rivers." Water research **32**(11): 3245-3260.

The USGS water science school (2014). "The effects of urbanization on water quality: Population growth."

Titirici, M.-M. and M. Antonietti (2010). "Chemistry and materials options of sustainable carbon materials made by hydrothermal carbonization." Chemical Society Reviews **39**(1): 103-116.

Titirici, M.-M., et al. (2007). "Back in the black: hydrothermal carbonization of plant material as an efficient chemical process to treat the CO 2 problem?" New Journal of Chemistry **31**(6): 787-789.

Tiwari, D. K., et al. (2008). "Application of Nanoparticles in Waste Water Treatment 1."

Tyagi, V. K. and S.-L. Lo (2013). "Sludge: A waste or renewable source for energy and resources recovery?" Renewable and Sustainable Energy Reviews **25**: 708-728.

Urase, T. and T. Kikuta (2005). "Separate estimation of adsorption and degradation of pharmaceutical substances and estrogens in the activated sludge process." Water research **39**(7): 1289-1300.

Vaccari, D. A. (2009). "Phosphorus: a looming crisis." Scientific American **300**(6): 54-59.

Wan Ngah, W. and M. Hanafiah (2008). "Removal of heavy metal ions from wastewater by chemically modified plant wastes as adsorbents: a review." Bioresource technology **99**(10): 3935-3948.

Wang, C., et al. (2012). "Graphene oxide stabilized polyethylene glycol for heat storage." Physical Chemistry Chemical Physics **14**(38): 13233-13238.

Wang, Y.-X. J., et al. (2001). "Superparamagnetic iron oxide contrast agents: physicochemical characteristics and applications in MR imaging." European radiology **11**(11): 2319-2331.

Wassel, R. A., et al. (2007). "Dispersion of super paramagnetic iron oxide nanoparticles in poly (d, l-lactide-co-glycolide) microparticles." Colloids and Surfaces A: Physicochemical and Engineering Aspects **292**(2): 125-130.

Weng, H.-X., et al. (2014). "Transformation of heavy metal speciation during sludge drying: Mechanistic insights." Journal of hazardous materials **265**: 96-103.

Wittmer, I., et al. (2010). "Significance of urban and agricultural land use for biocide and pesticide dynamics in surface waters." Water research **44**(9): 2850-2862.

World health Organization (2015). "Sanitation safty planning."

Xu, P., et al. (2012). "Use of iron oxide NMs in wastewater treatment: a review." Science of the Total Environment **424**: 1-10.

Yang, S.-T., et al. (2011). "Removal of methylene blue from aqueous solution by graphene oxide." Journal of colloid and interface science **359**(1): 24-29.

Yang, X., et al. (2009). "Superparamagnetic graphene oxide–Fe 3 O 4 nanoparticles hybrid for controlled targeted drug carriers." Journal of Materials Chemistry **19**(18): 2710-2714.

Zahm, S. H., and Ward, M.H. (1998). "Pesticides and childhood cancer."Environmental health perspectives **106**.Suppl 3 : 893.

Zenjari, B. and A. Nejmeddine (2001). "Impact of spreading olive mill wastewater on soil characteristics: laboratory experiments." Agronomie **21**(8): 749-755.

Zhang, W.-x. (2003). "Nanoscale iron particles for environmental remediation: an overview." Journal of nanoparticle Research **5**(3-4): 323-332.

Zhang, Z., et al. (2013). "Comparative study on adsorption of two cationic dyes by milled sugarcane bagasse." Industrial Crops and Products **42**: 41-49.

Zhao, G., et al. (2011). "Few-layered graphene oxide nanosheets as superior sorbents for heavy metal ion pollution management." Environmental science & technology **45**(24): 10454-10462.